Havforskningsinstituttet

METODIKKRAPPORT

Projekt: DABGRAF

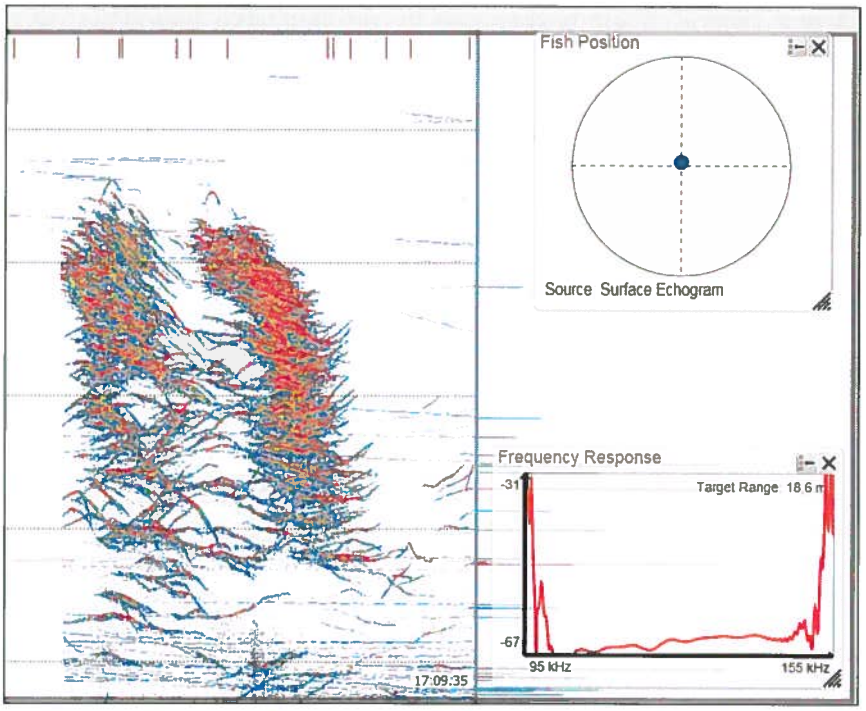

DOCUMENT INFO

Author(s)

Egil Ona

Classification

Open

Title:

Metodikkrapport

Denne rapporten gir beskrivelse av de akustiske metodene og prinsippene som ligger til grunn for utviklingen av DABGRAF programvaren. Den er skrevet på norsk i en stil som kan leses av mange, også ikke spesialister i akustikk. Der vi har brukt allerede publisert metodikk er det gitt i referanser, og hovedreferansene er vedlagt rapporten.

REVISIONS:

Rev.	Date	Author	Checked by:	Approved by	Reasons for revision
00	30.01.2017	Egil Ona	EO		

INNLEDNING

Hovedformålet med dette prosjektet er å utvikle programvare for størrelsesmåling av fisk ved bruk av nytt bredbånds ekkolodd teknologi.

Programvaren vil fokusere på å utvikle system for en horisontalt observerende bredbånds ekkolodd svinger, rettet inn i stimer på relativt kort rekkevidde fordi dette ofte er normalsituasjonen for fangsting med ringnot. En ønsker helst ikke å passere stimen med fartøyet fordi en da oppleve at stimen reagerer på fartøyet senere i fangstfasen.

I rapporten skiller en klart mellom fysiske problemer og biologiske, atferdsmessige problemer eller utfordringer.

Observasjoner, målinger og eksempler er gitt i andre rapporter i prosjektet.

Contents

Contents

Akustiske måleprinsipper for måling av fiskestørrelse

Det finnes grovt sett bare to måter å måle objektstørrelse med akustisk metodikk.

Den ene metoden er å belyse målet (stimen eller laget) med mange lave frekvenser over et stort frekvensspekter. For 20 – 30 år siden forsøkte en slik metodikk på blant annet sild i de såkalte Resonans i biomasse prosjektene, finansiert av NFFR og andre (Løvik & Hovem 1979). Målet var å generere lavfrekvent lyd over et spektrum som dekket resonansfrekvensen til fiskens svømmeblære. Kjennskap til relasjonen mellom resonansfrekvens og fiskestørrelse (egentlig svømmeblærestørrelse) ble så fiskestørrelsen beregnet ved inverteringsmetoder, som betyr at en sammenligner målingen med en modell for resonansegenskapene til fisken. Der målingen passer best med modellen gir tilpassningen ut en gitt størrelse.

Metoden har noe anvendelse innenfor planktonakustikk og partikkelakustikk, men mindre innefor fiskeriakustikk. Grunnen er rimelig klar. Det var vanskelig å produsere lavfrekvent utstyr med høy nok effekt til å sende fra 100 Hz til ca. 10 kHz. Både sender og mottaker ble svært store og relativt lite direktive (bred stråle = 30 til 60 grader). Videre viste det seg at selve biologien eller fysiologien til sild eller selve svømmeblærefunksjonen til sild var mer komplisert enn tidligere antatt. I samme stim, med samme fiskelengde var svømmeblærevolumet svært variabelt (Ona, 1990), og var dessuten avhengig av dypet silda stod på og også av individuelt fettinnhold.

Senere forsøk med lavfrekvent utstyr har vist lovende resultater på sild, men utstyret for å generere lyd-spekteret er komplisert og stort (og svært kostbart) (Godø et al., 2010, Stanton et al., 2010). Nøyaktigheten i størrelsesmålingen er dessuten antagelig for grov for fiskeriformål, der 2-3 cm nøyaktighet kreves, hvis metoden skal få betydning i en fangstfase. Forskere i fiskeriakustikk bør likevel følge med på utviklingen av svinger-teknologi innenfor militærakustikk og i bunnpenetrerende akustikk for å kontinuerlig vurdere om det går an å overføre slik teknologi til måling av fiskestørrelse med denne metoden.

Den andre akustiske metoden for størrelsesmåling er å måle ekkoet fra et og et enkelt individ mange ganger. For å kunne gjøre dette må en kunne" løse opp" registreringen slik at det oppstår et enkelt ekko fra et enkelt pulsvolum inne i ekkoloddstrålen. Dette volumet blir dannet av pulslengden benyttet i utsending og det arealet som strålen dekker på en gitt avstand. Normale pulslengder i fiskeriakustikk på de vanligste frekvensene er 1 millisekund, 1 ms, som med 1470 ms^{-1} lydhastighet gir en pulslengde i sjøen på 1,47 meter. Ekkolengden, eller lengden av ekkoet, målt på halvverdinivå (-3 dB), blir om lag halvparten av dette, eller ca 0,74 m langt på ekkogrammet. Siden ekkoloddstrålen for relativt dyre ekkoloddsvingere har om lag 7 graders åpningsvinkel, eller 0,122 radianer, så blir diameteren på strålen ca. 12 meter på 100 m, og arealet om lag 117 m^2. Pulsvolumet for en 1 ms puls blir derved 87 m^3 på 100 meters dyp eller avstand. Hvis målet skal oppfattes som et enkeltmål på denne avstanden må derved volumtettheten av fisk være veldig lav, for eksempel 1 fisk per 100 m^3 eller lavere. Torsk og annen bunnfisk opptrer som oftest i slike tettheter, og kan derved måles som enkeltfisk. Tettere forekomster vil måles som ekko fra multiple mål, eller flere mål i samme pulsvolum. For multiple mål er det kun flerfrekvensanalyse som i en viss grad kan indikere eller gi informasjon om målenes størrelse, mens ekkointegralet, som er summen av ekkobidragene fra alle målene inne i strålen er proporsjonal med fisketetthet.

Konklusjonen er altså at dersom denne metoden skal kunne brukes i tette forekomster, så må en endre pulslengde, og gjerne også strålebredde. Begge må endres rimelig mye for å få økt oppløsningen vesentlig. Videre, hvis det er mulig å løse opp forekomsten i enkeltekko, så er det videre ønskelig å kunne posisjonere målet inne i strålen for å korrigere for ulik effektivitet inne i strålen ved hjelp av splittstråle prinsippet. Dette prinsippet ble brukt fra om lag 1984 i vitenskaplige ekkolodd ES400, EK500 og EK60 og tilsvarende fiskeriversjoner, og er godt beskrevet i standard lærebøker i fiskeriakustikk, for eksempel Simmonds & MacLennan (2005); Ona et al., (1999), og vil ikke bli videre omtalt her. Bruk av splittstråle prinsippet gjorde det mulig å beregne reell målstyrke på oppløste mål direkte. Dette blir videre brukt til å indikere størrelsen av fisk fordi det er en rimelig bra sammenheng mellom målstyrke, TS, og fiskestørrelse. I fiskeri har denne informasjonen blitt brukt under tråling av torskefisk i lave tettheter, siden ekkoloddet ikke maktet å løse opp tettere forekomster. I de tilfeller ekkoloddet klarer å løse opp stimer med vanlig splittstråle ekkolodd er faren for feil (akseptering av ekko fra to eller flere fisk som om det kom fra en fisk) svært stor (se i Ona & Barange i Ona et al., 1999 og Sawada et al., 1993).

Nylig introduksjon av bredbånds ekkolodd, som ikke bare sender en enkelt frekvens, for eksempel 70 kHz med smal (5 kHz) båndbredde, men en puls som inneholder et "chirp" der frekvensen starter på en lav frekvens og ender på en høyere, for eksempel 50 kHz til 90 kHz, begrenset av svingerens kapasitet, gir muligheter for andre filtreringsmetoder enn før. Ny signalprosesseringsmetode; pulskompresjon metode som er en variant av «matched filter» metoden, der det motsatte ekkoene sammenlignes med det utsendte i en slags korrelasjonsmetodikk undertrykker da alle ekko der ekkospekteret ikke ligner det utsendte, og fremhever det som ligner. Grovt sett ser vi nå på en korrelasjonsmatrise i amplitude, heller enn en ren amplitude (Stanton & Chu 2010).
En bi-effekt av denne signalbehandlingen er en betydelig økning av oppløsingen radielt, eller i avstandsretningen, og lengden av ekkoet er nå bare 5% av utsendt pulslengde. Dess bredere bånd, dess finere oppløsning. Vi kunne nå, med standard bredbånds-svingere observere oppløste registreringer av stimer som vanlige ekkolodd bare viser som store røde klumper. Stimer av sei (som ikke er veldig tette) kunne oppløses på om lag 100 m avstand. I tillegg til økt oppløsning kunne en videre utføre en FFT (Fast Fourier Transformasjon) analyse over selve ekkoet av enkeltindivider, og hente ut frekvensspekteret av målet.

I et tidligere NFR prosjekt ble det utført studier av ekko-oppløsning, og kalibrering av prototyper av dette ekkoloddet på ulike frekvenser, som konkluderte med at ekkoloddet kunne kalibreres like nøyaktig i hele spekteret som for smalbåndsekkolodd, 0.1 dB, eller ± 2% nøyaktighet. Videre ble det vist at en også kunne kalibrere stråleform for splittstråle ekkolodd som funksjon av frekvens innenfor den største delen av hovedloben i ekkoloddstrålen. Dette var et godt utgangspunkt for DABGRAF prosjektet.

Kort oppsummert har DABGRAF prosjektet utført datainnsamling på 5 tokt, og 2 felteksperiment i Austevoll der utstyr og personell dedikert til dette prosjektet har deltatt. (Se egen datarapport [1]). DABGRAF målingene har blitt utført på tokt der hovedformålet med toktet var delt mellom CRISP prosjektet og DABGRAF prosjektet. Fra HI har Egil Ona, Gavin Macaulay, Rolf Korneliussen og Atle Totland deltatt for DABGRAF – prosjektet.
Videre har CMR hatt ansvaret for utvikling av programvaren for størrelsesmåling, for bearbeiding av utvalgte datasett fra innsamlingen, og for utprøving av programvaren. På CMR har Armin Pobizer vært prosjektleder, mens seniorforskerne Yngve Hegglund og Inge Elliassen også har vært involvert.

Spesifikasjonen av programvaren har blitt utført av prosjekt-teamet i samarbeid, og her har også Rolf Korneliussen fra HI bidratt i prosjektet.

Kongsberg / Simrad har bidratt i prosjektet ved utlån av prototype EK80 ekkolodd, og på beregninger og konstruksjon av ny smalstråle svinger.
Eksperiment-plattformen som den nye svingeren har blitt montert i er konstruert av CFLOW, 6030 Langevåg, og tilt/pan motor for svingeren er innkjøpt fra Ocean Tools Ltd, Scotland.

Tegninger og design for en eventuell permanent montasje på fiskefartøy er utført av METAS A/S, Bergen, ved Terje Torkelsen.

Metodikk- beskrivelse, grovt

Enkeltfisk-deteksjon-splittstråle

Gitt et enkelt mål, detektert 100 meter fra fartøyet i sidemontert standard 7° splittsstråle svinger. Med høg pingrate vil samme mål bli målt flere ganger idet fartøyet beveger seg framover, og vi får en typisk enkeltfiskspor eller et ekkotrace. I utvalgte deler av registreringen der en ser slike enkeltfiskspor kan en måle ekkostyrke og ekkospekter av enkelt-individer. Vi må videre anta at disse er representative også for de som ikke er oppløst (blanda ekko fra flere individ).

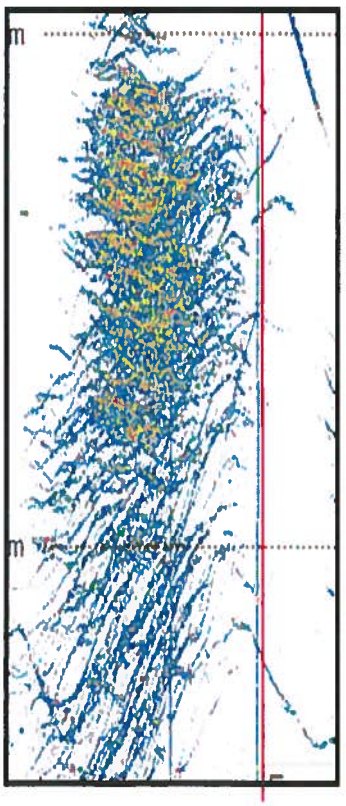

Figur 1. Eksempel på enkeltfisk spor av sild i en sildestim fra 2012 toktet

Med bredbåndsekkolodd registreres først hver deteksjon av enkeltfisk nedover i vannsøyla i hvert ping, angitt ved en rød strek. Hvert ping er uavhengige, etter hverandre, og dataene i hvert ping henger ikke sammen. DABGRAF prosjektet må først lese inn data for hvert ping, og sette disse sammen for å vurdere om de henger sammen i et ekkotrace. Dette er utført i henhold til målfølgings (target tracking) algoritmer tidligere beskrevet i for eksempel Brede et al., (1991) og Handegard (2007). I DABGRAF har vi brukt metoder og matematikk fra Handegard (2007). Artikkelen er vedlagt istedenfor å repetere innholdet her. Prinsippet består i at en åpner et vindu i rommet rundt en allerede detektert mål, og så undersøker en om det kommer nye, sannsynlige deteksjoner av samme mål innenfor dette vinduet, og så videre. Etter noen få deteksjoner kjenner en både signalstyrke og målets bevegelsesretning, og kan da sette nye kriterier for ny deteksjon, for eksempel på retning og fart, siden fisken ikke kan plutselig forandre retning og fart. Målfølging, der svingeren også beveger seg, som her, øker kompleksiteten i målfølgingen.

Lesealgoritmer EK80

For å kunne vise fiskestørrelse i reell tid må lesealgoritmer i DABGRAF programmet derfor lese med samme hastighet som dataene blir skrevet av EK80, og dette var første bøygen i prosjektet fordi EK80 leverte 507 ganger så mye data som EK60 per tidsenhet, og selv nye datamaskiner hadde problemer med dette. Se egen rapport på dette fra CMR, [2] der en tidlig i prosjektet vurderte om dette var mulig. Konklusjonen var at med moderne datamaskiner med flere kjerner og raske disker var dette mulig.

Fartøyets koordinatsystem

Videre har fartøyet (og svingeren) sitt eget koordinatsystem, slik at et mål som blir registrert i et visst dyp og avstand og posisjon, i neste øyeblikk blir registrert i en annen posisjon hvis en ikke korrigerer for fartøyet og svingerens bevegelse. En MRU (Motion reference unit) om bord på fartøyet registrerer posisjon, rull, pitch og heave av båten (og beregnet til svingeren). Hvis MRU leses med full hastighet, 10Hz, så vil en greie å kompensere for dette (se også Handegard 2007, som kompenserte for svingerens bevegelse, med samme matematikk, men med en annen metodikk, fordi han ikke hadde MRU på svingeren).

Fiskens koordinatsystem

Hvis vi nå går over i fisken sitt koordinatsystem, så er det kjent at ekkorefleksjonen (og ekkospekteret) er svært avhengig av hvordan den er observert. Fisken har sitt eget direktivitets-mønster, som særlig her på relativt høye frekvenser, er ekkoet sterkt i rent sideaspekt (broadside) og kraftig redusert, kanskje med 20 dB, eller 1/100, når fisken blir sett forfra eller bakfra.
Dette må vi ta hensyn til, og ville først bruke en akustisk-matematisk modell for ekkorefleksjon av en typisk sild, for videre å sammenligne ekkorefleksjonen med målingene. Koordinatsystemet er vist i Figur 2.

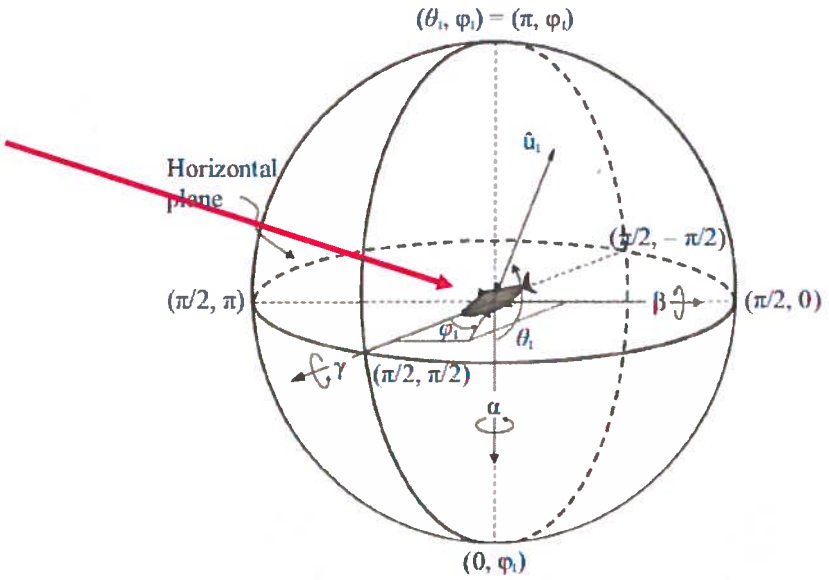

Figur 2. Koordinatsystem for en enkelt fisk i rommet (fra Kimura et al., 2011, med typisk innsyns-retning (rød) for et sidemontert ekkolodd

For en enkelt frekvens kan vi da beregne ekkorefleksjon fra en prolat sfæroide som har samme form som svømmeblæren i sild, og sammenligne den med en aktuell måling på denne frekvensen. Figur 3 viser typisk direktivitet, som er ekkorefleksjon som funksjon av rotasjonsvinkel for en enkelt sild på en frekvens, 200 kHz. Figuren viser både en komplisert matematisk beregning, og rene målinger. Husk at figuren er gitt i dB, som er logaritmisk. Dette betyr at minus 10 dB er 1/10 og -20 dB er 1/100 i amplitude. Som vi klart ser er ekkoet sterkest når vi ser silda rett fra siden, 0° og 180°, og den er tosidig symmetrisk. Den er fremdeles sterk, med en målstyrke på om lag -30 dB selv om den vrir seg ± 10 grader i forhold til innsyns-vinkelen, men faller kraftig, 10 – 20 dB, når vinkelen øker utover 10 grader. Når vi ser silda rett forfra eller bakfra, 90° eller 270°, er ekkoet redusert til under 1/100 del, eller -20 til -25 dB.

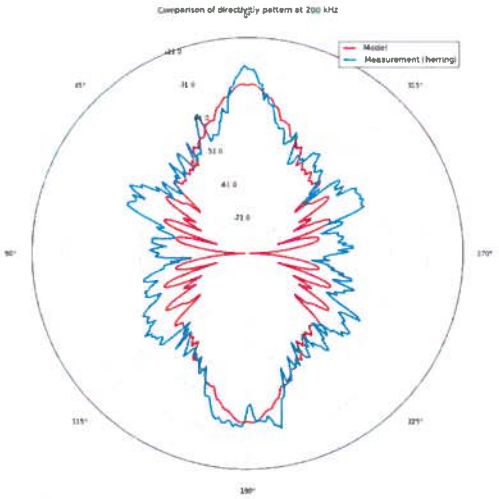

Figur 3. Direktivitetsmønster for sild (33 cm) beregnet matematisk (rød) og målt på 200 kHz, målt ved å rotere silda 360 grader i sideaspekt

I første del av DABGRAF prosjektet var planen å bruke en modellbasert tilnærming, den målingene ble sammenlignet med en modell av ekkorefleksjonen. Planen for dette var å bruke en komplisert svømmebæremodell og beregne denne modellen for alle størrelseskombinasjoner og rotasjoner. Modellen ble beregnet av Gavin Macaulay, og er en kombinasjonsmodell for beregning av ekkoet fra svømmeblæren til sild, beskrevet som en prolat sfæroide. Resultatet fra modellen er vist i figur 4.

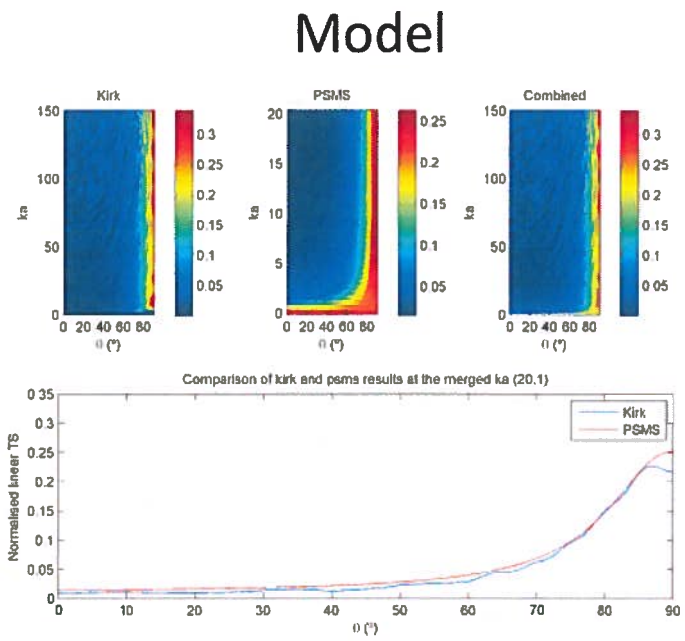

Figur 4. Modellen for å beskrive ekkorefleksjon fra sild som funksjon av frekvens (ka) og rotasjonsvinkel, som var utgangspunktet i starten av DABGRAF prosjektet. 90 grader er her direkte sideaspekt og 0 grader er imot hodet. Siden ekkoet er symmetrisk er bare den ene siden vist. Utgangspunktet for denne ble publisert under DABGRAF prosjektet fordi det var en del uklarheter om hvilken matematisk modell (av 5-6 alternativer) som best kunne beskrive ekkoet fra en slik kropp under full rotasjon, som vi hadde behov for (Macaulay et al., 2013).

Forsøk med modellbasert minimalisering

I starten av DABGRAF prosjektet skulle en måle ekkostyrke, og målets orienteringsvinkel og finne beste tilpasning med ekkomodellen for sild og makrell. For sild er det svømmeblæren som er ansvarlig for 90% av ekkoet og det er derfor svømmeblærelengden som er målet med minimaliseringen, og fiskelengde for makrell, men en tilsvarende modell for makrellkroppen. Det viste seg at denne måten å gjøre det på lett gav multiple løsninger, dvs. samme måling kunne gi flere likeverdige svar. Figuren under viser dette, at en har 2 eller 3 like sannsynlige lengder for samme måling under 0 – 90 graders rotasjon av fisken. En bestemte derfor at istedenfor en modellbasert matrise av ekkorefleksjon av sild burde en måle enkeltsild i det ekkospekteret en hadde tenkt å bruke, for så bruke disse dataene for å trekke ut informasjon

om størrelse, direkte. Siden det ikke finnes slike data fra før måtte en gjennomføre en slik måling / analyse selv i regi av DABGRAF prosjektet.

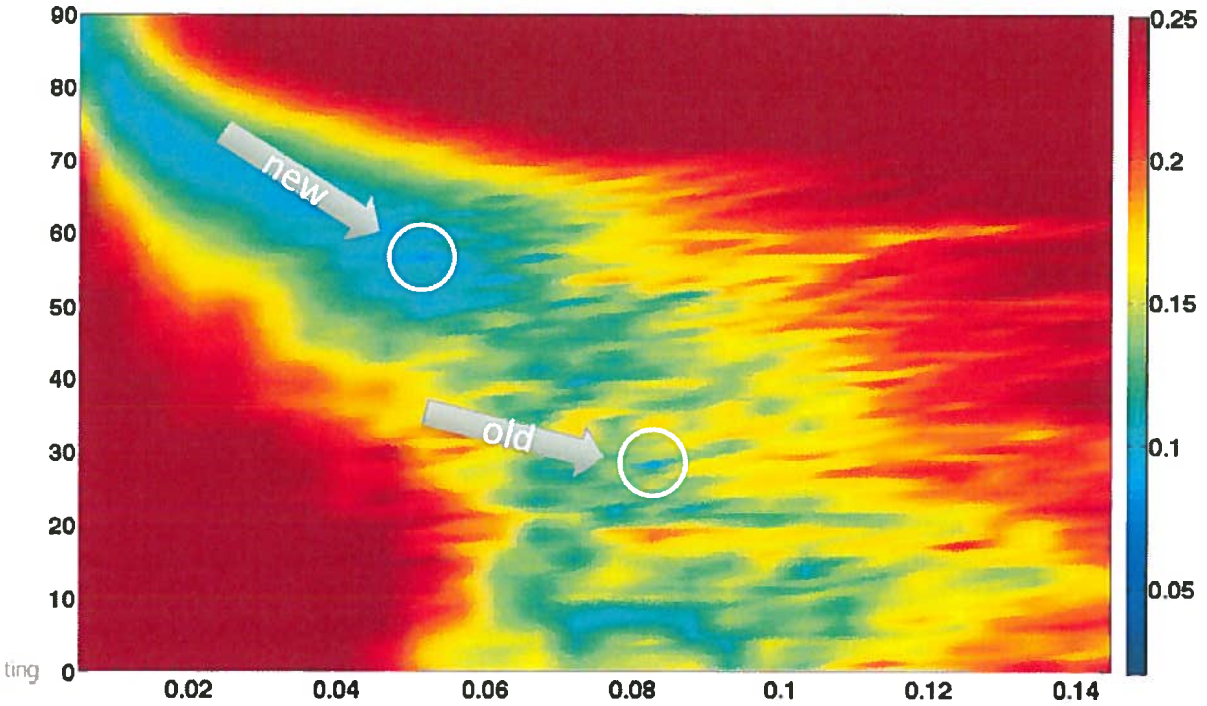

Fig 5. Feilfunksjon (høyre akse) for beregning av svømmeblære lengde (korrekt = 8 cm, = 0.08 m) som funksjon av rotasjonvinkel. Prinsippet, minst feil, blå farge gir best løsning. Problemer med multiple løsninger er klart, her kan det enten være en sild med 8 cm svømmeblærelengde = 32 cm sild, eller like godt en med 5 cm svømmeblærelengde. Løsningene oppstår ved ulike rotasjonsvinkler.

Direkte målinger av fiskens direktivitet, 170 – 270 kHz

Siden vi fant at det var store avvik mellom målt direktivitet og modellert direktivitet ønsket vi derfor å bruke målt direktivitet som utgangspunkt i DABGRAF. Dette kompliserte prosjektet betydelig, fordi det finnes svært få målinger av dette i bredbånds-modus, og målingene måtte utføres i selve prosjektet. 25 sild og 10 makrell ble målt på denne måten ved havbruksstasjonen i Austevoll, i et eget måleoppsett (Figur 6), der selve måleoppsett med rotasjonsenhet, datastyring og synkroniseringsenhet med EK80 ekkoloddet ble bygget ved verkstedet på HI og av Atle Totland, HI. (Se egen DABGRAF rapport til FHF).
Vi kunne da kun måle på fisk som var tilgjengelig på stasjonen fra andre prosjekter, og dette begrenset oss kun til målinger på stor, voksen sild (28-35 cm) og makrell (34-37 cm), mens vi gjerne skulle ha målt dette over et mye større lengdespekter for begge arter. Slike målinger blir utført i et nytt NFR prosjekt fra 2016 – 2020.

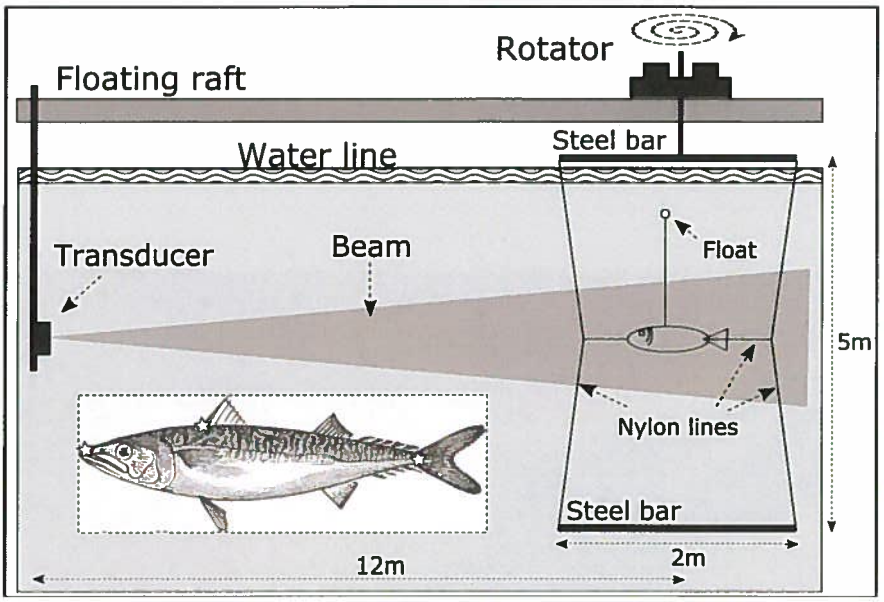

Figur 6. Rotasjons-enhet for å måle fiskens direktivitet i sideaspekt med bredbånds ekkolodd. Fisken er bedøvd rett før måling og opphengt som vist, rett etter overføring fra lagringsmerd.

Siden vi bruker bredbåndsekkolodd får vi et mer nyansert bilde av direktivitet, siden vi måler over mange frekvenser samtidig.
Det egentlig målte direktivitets-mønsteret fra en sild, målt kontrollert i Austevoll er vist i Figur 7.
Denne viser at direktiviteten følger et mønster, med skarpere direktivitet med økende frekvens.

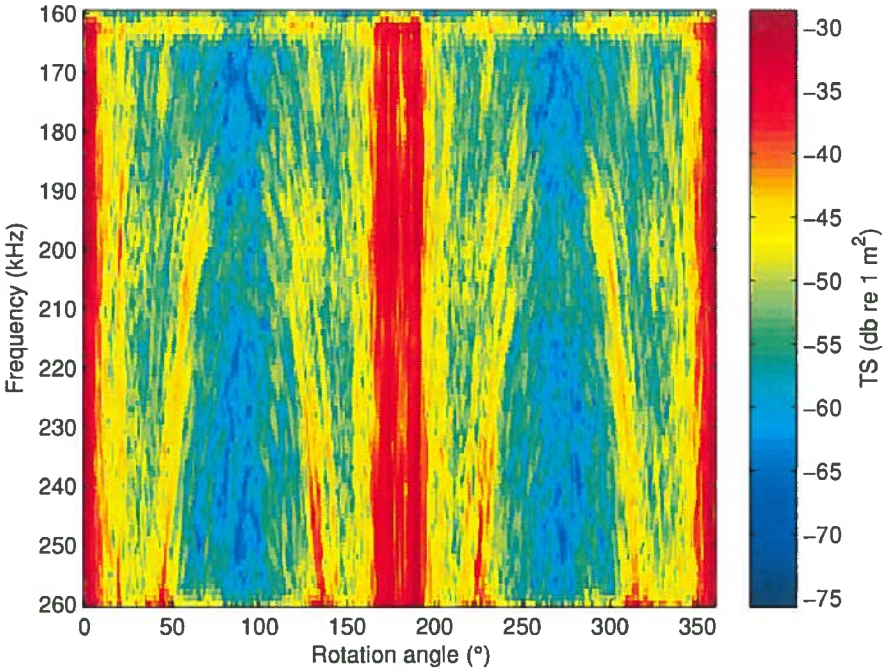

Figur 7. Målt direktivitetsmønster av sild (33 cm) som funksjon av frekvens fra 160-260 kHz. Rotasjonsvinkel er vist langs x-aksen fra 0 grader(sideveis) gjennom alle vinkler til 180 grader (andre bredside) og videre tilbake til første bredside (360 grader). Ekkostyrke, TS er vist i fargeskalaen -30 til -75 dB. Siden ekkoet i full bredside er om lag -30 dB, og fra hale og hode (90 og 270 grader) er under -60 dB, tilsvarer dette en lineær skala på 1/1000. Ekkoet for silda sett fra siden er over 1000 ganger sterkere enn fra hode/hale i nesten hele frekvensbåndet. Merk at plasseringen av sidelobene, eller avstanden mellom sidelober og hovedlobe er frekvensavhengige, og sterkere på høyere frekvenser.

Med disse målingene kunne en nå hente ut data, og beregne funksjoner for størrelsesavhengighet basert på tre parametere: Ekkostyrke, frekvens-spekter og puls-strekking.

Ekkostyrke eller målstyrke (Metode 1)

Denne parameteren kjenner vi rimelig godt til i fra kontrollerte målinger og modellering av ekkorefleksjon. En antar at denne går som: TS = $20\log_{10}(L) - 67$ dB, for middelekkoet av sild, som gir TS = -35.0 dB for en 40 cm lang sild og TS = -41.0 dB for en 20 cm lang sild. Dette betyr at det er 6 dB forskjell i middelekko, eller en faktor på 4 i lineær skala. Det betyr at ekkoet fra en 40 cm sild er 4 ganger så stort som ekkoet fra en 20 cm sild. Dette gir oss en oppløsningsgrad på 6/20, eller 0.3 dB/cm. Ytterligere kjenner vi også en mer kompleks modell for ekkorefleksjon fra sild, som også inneholder et trykk-ledd, slik at en korreksjon for dypet silda befinner seg på er tatt hensyn til.
Siden spredningen i ekkostyrke fra sild sett fra siden (eller ovenfra) er om lag 30 dB, er det vanskelig å oppdage en endring på noen få centimeter uten å måle mange ganger. Etter 100 eller kanskje 1000 målinger stabiliserer middelverdien seg, og en kan da hente ut størrelsesindikatorene. Dette er det som også blir gjort med nåværende splittstråle ekkolodd, men med stor spredning i størrelse. Middelverdien er likevel en rimelig stabil verdi, og ofte bruker en robust middelverdi, eller modal verdi der sjansen for at enkelte feilmålinger påvirker middelverdien er lavere.

Spektralanalyse (Metode 2)

Ekkospekteret fra enkeltfisk endrer seg med størrelse, fra et noenlunde flatt spekter for mindre fisk, til et komplekst spekter for større fisk. Særlig vil interferens mellom lydbølgene som reflekteres fra objektet direkte og den lyden som trenger inn i dyret og reflekteres fra undersiden (buksiden) og de som går rundt dyret skape spesielle mønster med konstruktiv og destruktiv interferens. For ekko fra metallkuler ser en ofte etter slike mønster, som er avhengig av lydhastighet og tetthet av kulen, og av diameteren. Dersom en kjenner eksakt diameter, materiale og to lydhastigheter inne i kulen kan man beregne spekteret eksakt. På samme måte kan en lete etter tilsvarende effekter på fisk, som i praksis er tilsvarende mål som metallkuler, men med en annen form og tetthet.

Det teoretiske grunnlaget for dette ble lagt av Chu & Stanton i 1998, som arbeidet med ekko fra dyreplankton men for ekkorefleksjon fra enkeltfisk ser det slik ut:

Frekvens domenet

Eksempel: Atlantic Mackerel (*Scomber scombrus*)

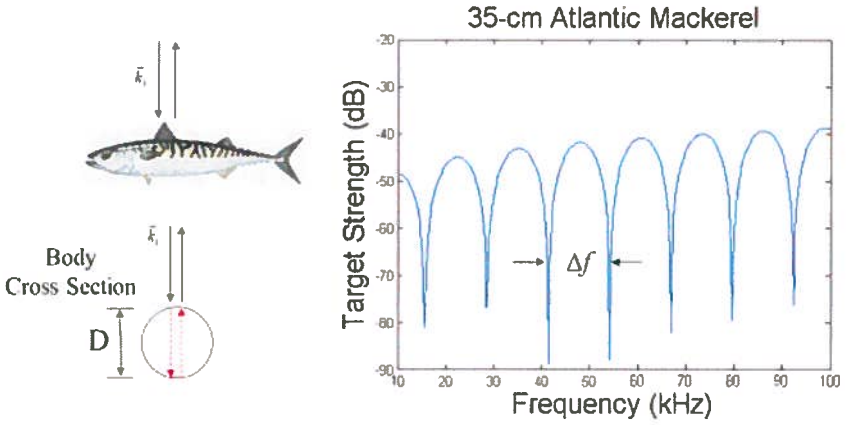

Figur 7. Ekkostyrke (TS) som som funksjon av frekvens som viser mønsteret med nullpunkt i frekvensdomenet på høyere frekvenser, som indikerer at for et objekt med en viss diameter, med en viss tetthet, så vil avstanden mellom nullpunktene (Δf) kunne måles og relateres til objektets størrelse.

Videre foreslår Chu, basert på modellering, under DABGRAF toktet i 2014, se vedlegg, (Chu 2014) at relasjonen vil gå om lag slik for typisk fiskekjøtt-mål:

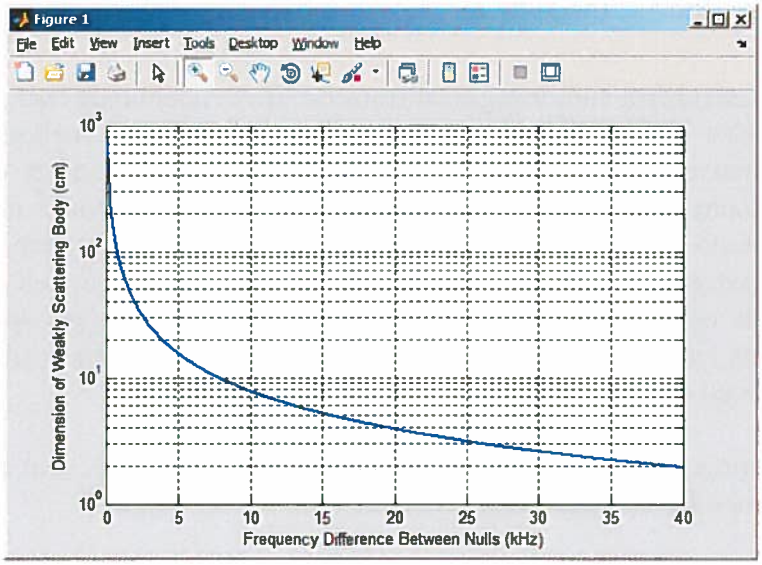

Figur 8. Forholdet mellom dimensjon på objektet (cm på y-aksen) og frekvensdifferanse (i kHz) mellom null-punkt i spekteret for typisk fiske-kjøtt. Siden vi her ser etter dimensjoner på 3 cm til 40 cm, må vi her se etter slike avstander mellom nullpunkt på 2-20 kHz. Dess lavere differansefrekvens, dess større er individet.

Materialet samlet inn i Austevoll på enkeltfisk er analysert for slike sammenhenger, og selv om lengdespredningen i vårt materiale er liten, finner Pobizer (CMR 2013) en svak sammenheng med størrelse, og dette blir lagt inn som måleparameter i systemet. For å

virkelig utforske dette, burde vi ha målt både sild og makrell fra 10 cm til 38/40 cm, målt enkeltvis.

Måling av puls-strekking (Metode 3)

Siden bredbåndsekkoloddet har langt høyere oppløsing i dataene enn eldre ekkolodd, og oppløsningen radielt er 3 millimeter, og hele ekkoet om lag 7 cm langt, er det faktisk mulig å måle effekten av målets størrelse orientering på lengden av pulsen. Dette ble beskrevet av Stanton et al., (2003), som brukte denne metoden til å måle orienteringen av fisk.

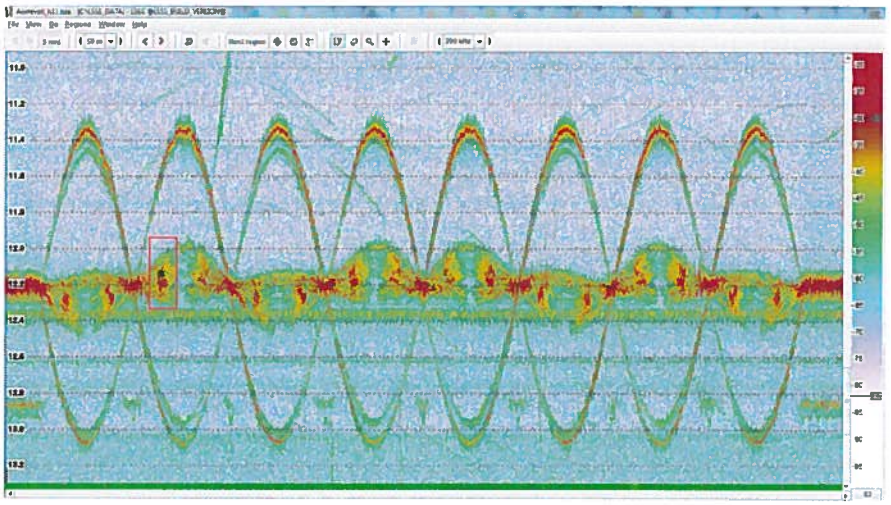

Figur 9, ekkolengde av en 34 cm sild under full rotasjon flere ganger. Inne i den røde boksen kan en analysere strekkingen av ekkoet som funksjon av rotasjonsvinkel. Hver bue er 180°, og ytterbuene er bare ekkoet av opphengings-systemer (nylongut) til fisken, og skal ikke analyseres. (se egen DABGRAF rapport).

Stanton sine forsøk indikerte at puls- stekkingen var relatert til lengden av objektet (fisken) og rotasjonsvinkelen på følgende måte.

$$\Delta t = \frac{2L_{eff}}{c}\left|\cos(\phi)\right|$$

Hvis en kjenner fiskelengden, som Stanton, kan han da beregne orienteringsvinkelen ved å måle Δt. Vi har bare snudd problemet på hodet, siden vi måler, Δt, vi beregner orientering (fra målfølging, slik at vi kjenner målets orientering, og kan derved estimere $L_{eff,,}$ eller lengden på objektet, fiskelengde.

Forsøkene på denne målingen, utført på data fra Austevoll er vist i rapporter fra CMR, men jeg viser her et eksempel, som viser at vi faktisk har bedre data på dette enn det Stanton hadde i sitt originale arbeid: (Stanton et al.,2003);

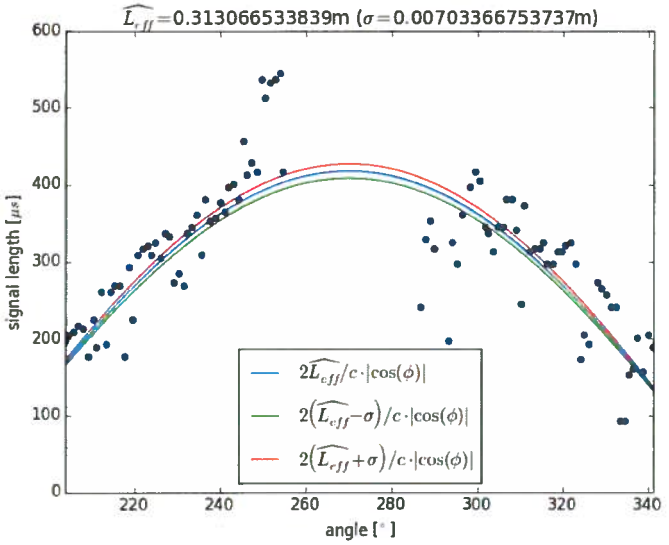

Figur 10. Målinger av pulsens lengde, og strekking som funksjon av rotasjonsvinkel for en 32 cm sild. Effektiv lengde er her estimert til 31. 3 cm (se øverst), med god nøyaktighet. For rotasjonsvinkler rundt 270 grader (bredside), kan en ikke måle effekten av puls-strekking nøyaktig nok, og en må derfor velge enkeltfisk med ugunstig orientering for en slik måling. (se ellers egen rapport fra CMR 2013: Size inversion metholology).

Videre har en i dokumentet CMR 2013, Size inversion methodology undersøkt nøyaktigheten av denne målemetoden, og funnet at den er best på mål som ikke har bredside orentering, og at denne bare blir brukt på de målene.

Oppsummering av måleparametre

Vi har nå tre parametre som estimerer fiskens størrelse. Målstyrke (TS) (Metode 1), Effektiv lengde målt fra Stanton sin metode (L_{eff}) (Metode 3), og objektsstørrelse målt fra avstand mellom nullpunkt i ekkospekteret (Metode 2). Hvordan man skal tillegge disse vekt for å bestemme seg for en bestemt lenge baserer seg på Pobizer et al., (2015). Prinsippet baserer seg på å bruke hver av måleparametrene og beregne sannsynligheten for at fisken er en gitt lengde, for eksempel 30 cm, og så oppsummere mange målinger i en sannsynlighetsfordeling. Det er denne sannsynlighetsfordelingen som blir vist i displayet til fiskeren i DABGRAF - programmet.

Selve målemetodikken i DABGRAF

Mye av styrken i DABGRAF prosjektet ligger i den nye målemetodikken, delvis utviklet i prosjektet. Selve bredbånds-ekkoloddet var under utvikling i NFR prosjektet WESTZOO, og vi har i DABGRAF brukt prototyper av ekkoloddet EK80. Fra høsten 2016 er dette ekkoloddet ferdig utviklet, og er nå i kommersielt salg. I 2015 og 2016 (Etter at DABGRAF egentlig var ferdig som prosjekt) har vi brukt den kommersielle versjonen av EK80 i samme oppkopling for forsøk. (De tidligste forsøkene med standard svingere, som viste seg å gi for dårlig volumoppløsning, og videre spesialutvikling av en svært smalstrålet svinger for prosjekter er beskrevet tidligere i rapporter fra HI, og vil ikke bli beskrevet her.)
Den endelige, eksperimentelle svinger-oppsettet (for forskning) som nå har blitt brukt er vist i Figur 11. Denne forskningsmonteringen som bare kan monteres på FF «G.O. Sars» sin senkekjøl fordi den kan trekkes inn over vannoverflaten inne i fartøyet, og utstyret monteres (ca. 5 timer, 3 mann) til hvert DABGRAF tokt, har gitt oss unike muligheter til å måle enkeltfisk både fra ryggsiden (dorsal) og fra siden, - som var den ønskede måten fiskerne ville måle fisken i en kaste-situasjon. Svingeren kan her ved hjelp av den tunge tilt/pan motoren, roteres i steg på 1 grad fra sideaspekt, horisontalt, til loddrett i løpet av sekunder. En kan også peke skrått nedover med for eksempel -10 graders tilt, dersom fisken står på 50 m dyp, tilsvarende som for sonar. Den ekstra, vesle kjølen er montert bare en beskyttelse for tilt/pan motoren, som her må stå fast og holde posisjon i 10 knops fart uten motor, og for å redusere støy fra turbulent strøm over flatene, og vil ikke være nødvendig ved en stan ardisert montasje.

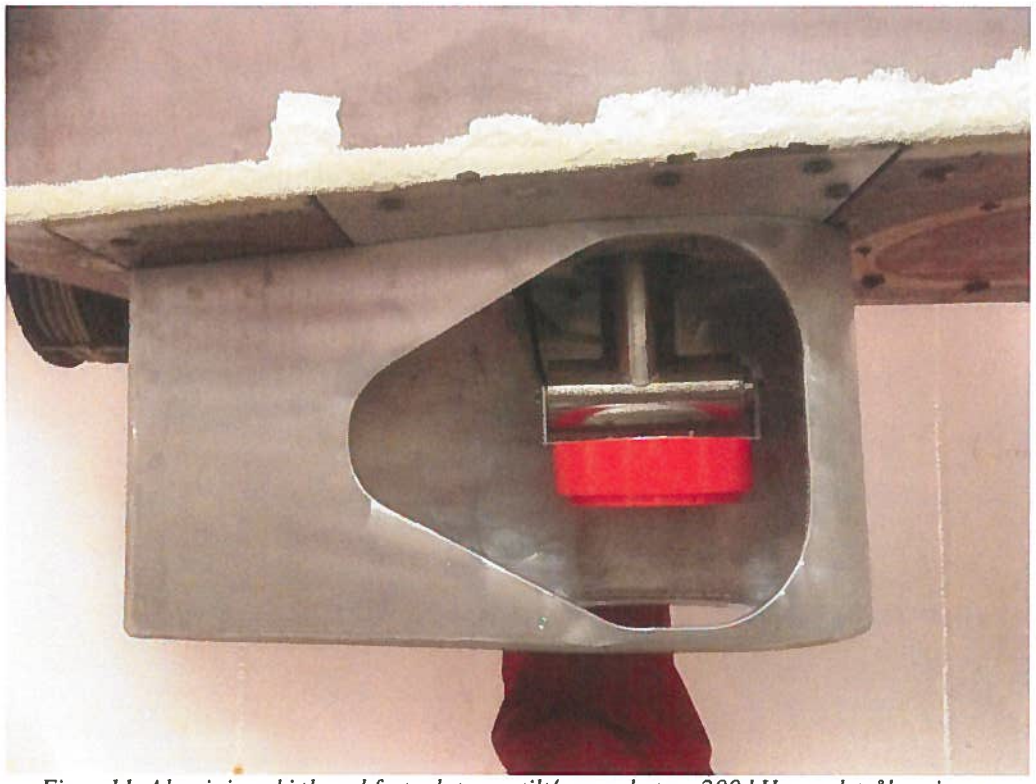

Figur 11. Aluminiumskjøl med festeplate, ny tilt/pan enhet og 200 kHz smalstråle svinger.

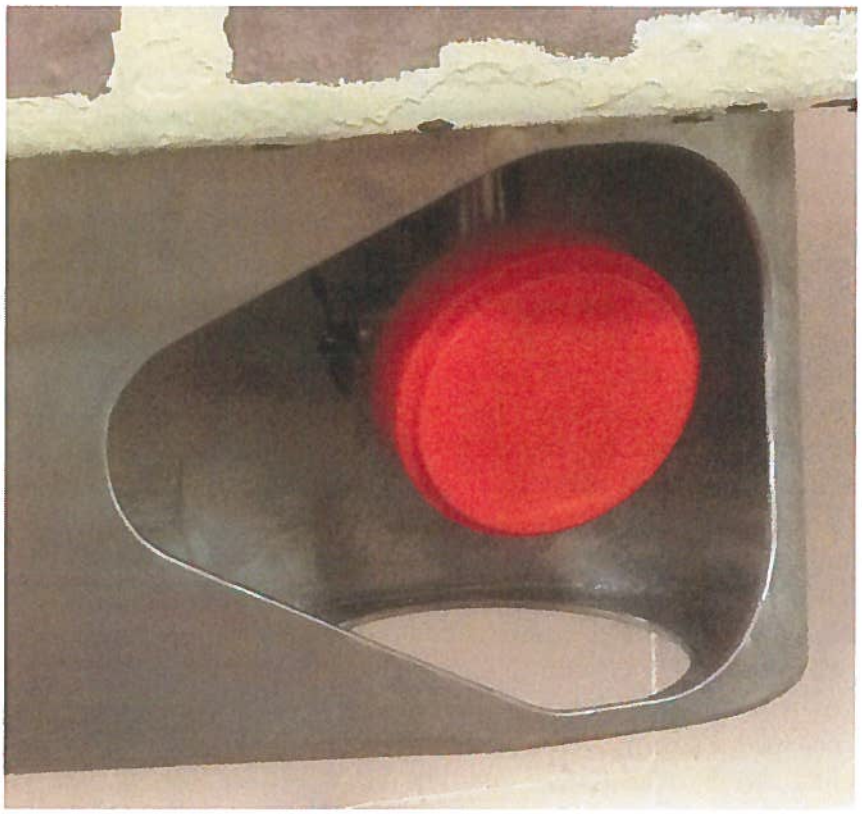

Figur 12. Svinger rotert til – 10 grader nedover, relativt overflaten.

Dataopptak med ny montasje.

Det er utført datainnsamling med ny svinger montasje på tre tokt, hvorav to tokt er utført etter egentlig DABGRAF prosjektets avslutning.
Data fra sideveis og nedover rettet smalstråle EK80 svinger ble innsamlet kontinuerlig, og viste god oppløsningsevne i begge aspekt på typiske makrellkonsentrasjoner på fiskefeltet. I kommersielle konsentrasjoner av makrell viste systemet at vi kunne oppløse og størrelsesmåle makrell fra 10 – 100 meter fra svingeren (se under), og til 50 – 60 meters dyp i veldig tette konsentrasjoner. Noen eksempler på oppløsningen er vist under.

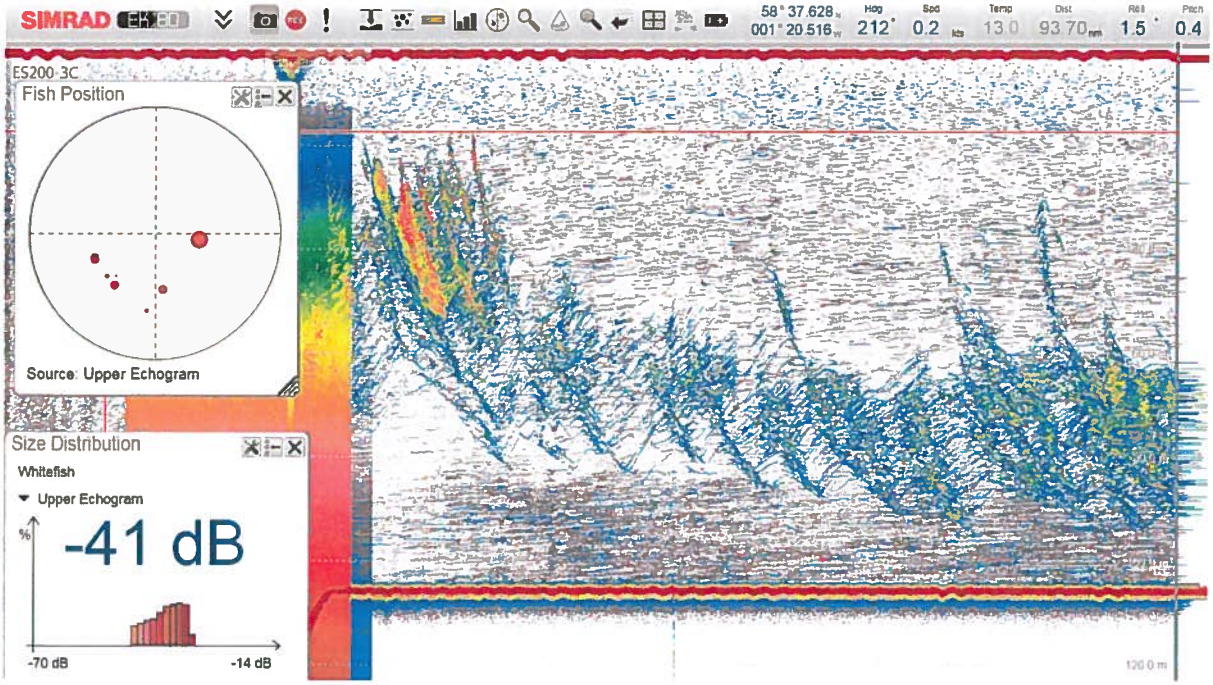

Figur 13. Oppløst makrell-lag som tydelig viser veldig aktiv makrell som svømmer hurtig opp og ned i vannsøyla i grupper på 10 – 100 enkeltindivider med samme atferd. Størrelsesmåling mulig her helt til bunnen på 100 m.

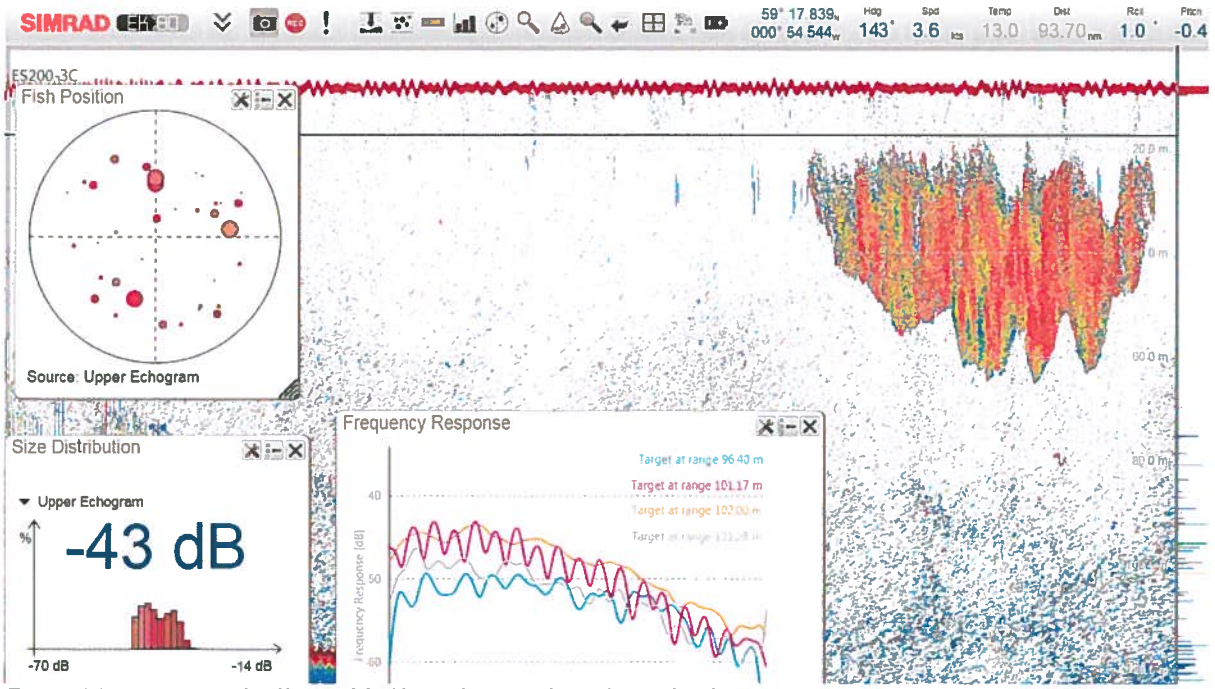

Figur 14. Tettere makrellstim 20-60 m dyp, med oppløste forekomster i toppen av stimen. Størrelsesmåling mulig.

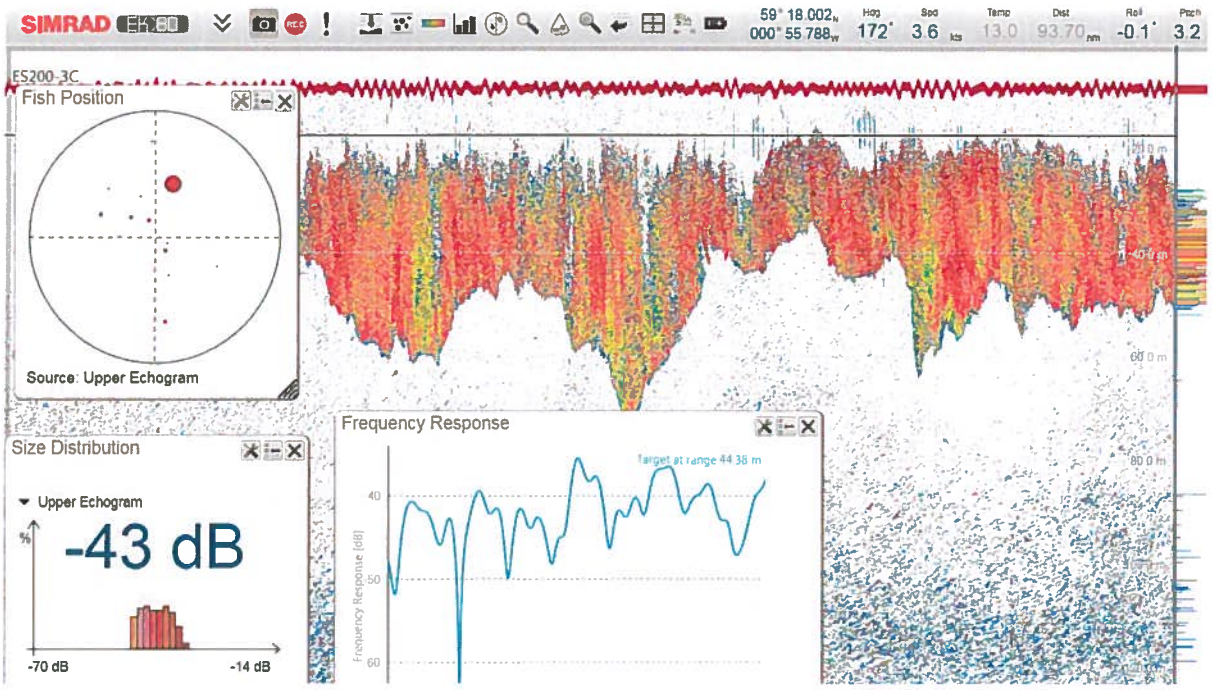

Figur 15. Kompakt lag av makrell, oppløsning og størrelsesmåling mulig bare i toppen av laget.

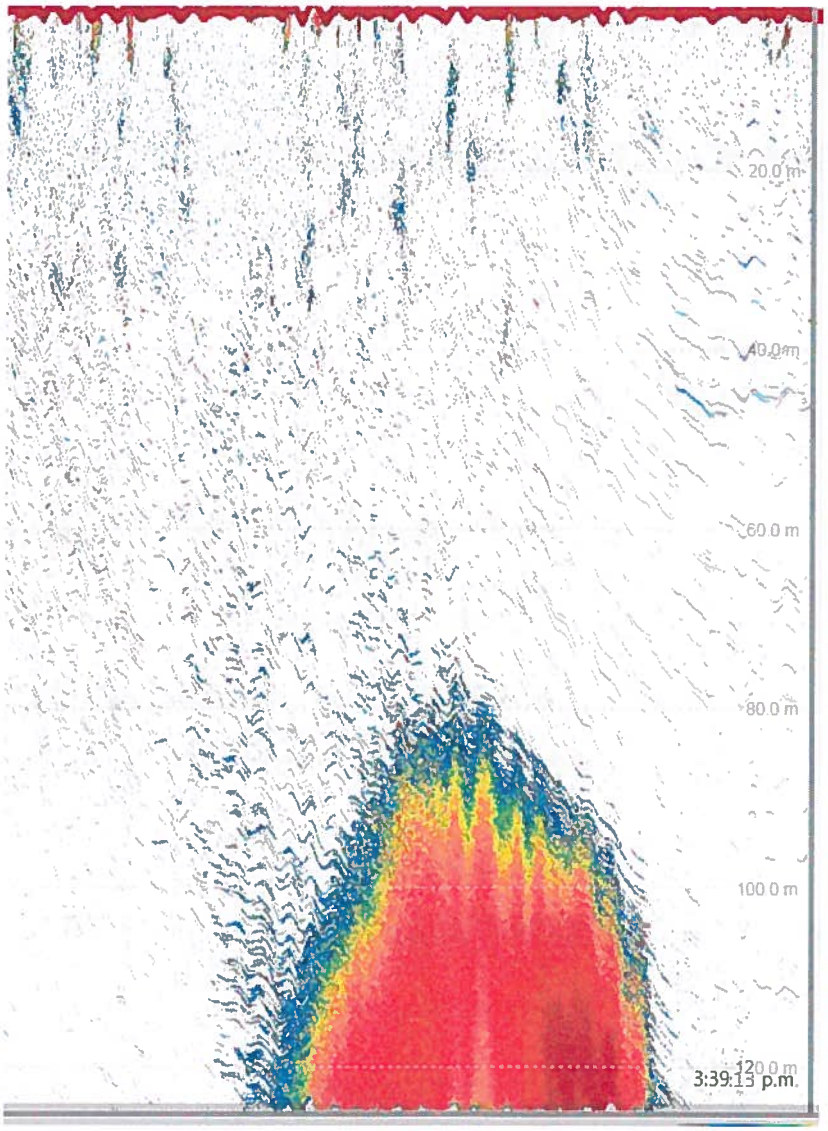

Figur 16. Tett makrellstim på 80 – 100 m, med oppløste enkeltfisk i utkanten av stimen.

Forsøk på reell tids visning med DABGRAF programvare og maskin

Etter at DABGRAF programvaren var ferdig fra CMR har vi utført forsøk med reell visning fra en nyinnkjøpt datamaskin i stor skjerm, direkte montert på broen på FF «G.O. Sars» i 2015. Datamaskinen viser data fra EK80 direkte, og bropersonellet kan bruke DABGRAF direkte, og ved enkel opplæring ble de vist hvordan de skulle operer systemet. En demofilm av hvordan DABGRAF måler og viser størrelse, og mulighetene for å velge ut og forstørre områder på skjermen er vist steg for steg. Videre oppkopling av dette systemet vil bli utført i 2016-toktet, også for innsamling og validering av selve størrelsesmålingen.
Rett under er det vist noen bilder fra slik uttesting på makrell, men for å vurdere programsystemet, virkemåte og settinger henvises det til demofilm, og reell oppkopling vist på for fiskere og andre interesserte på FHF/HI/FDIR «Seminar for den pelagiske flåten», Flesland Bergen 15.12 2015, der både demofilm og systemet var fullt oppkoplet med demo

direkte fra ekkolodd som kjørte avspilling av reelle data i sanntids fart. Mange fiskere var begeistret for denne muligheten, og ønsket lykke til med testingen.

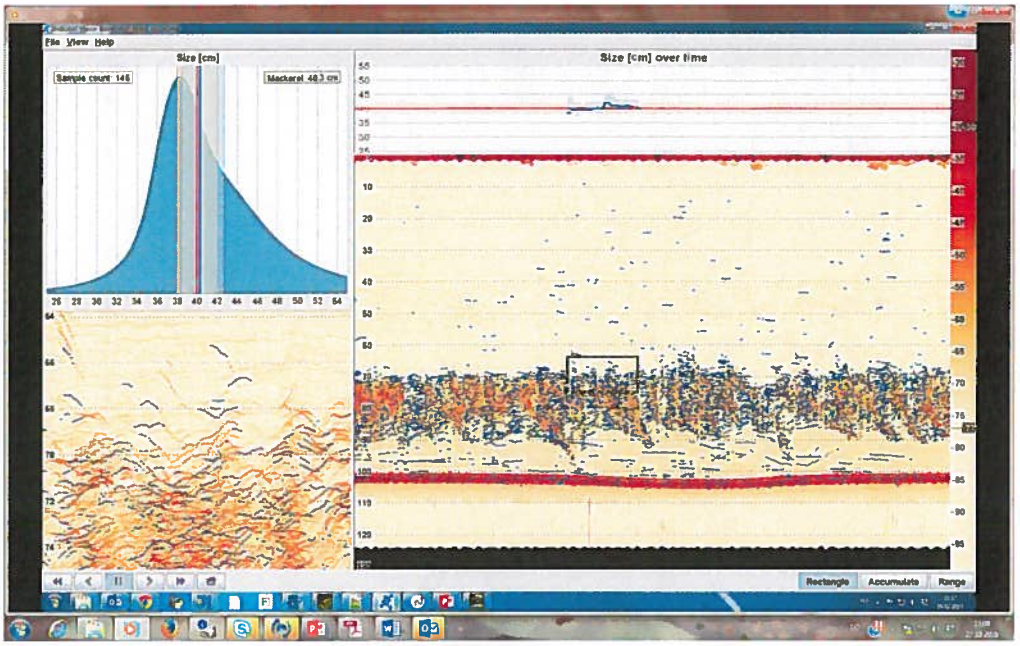

Figur 17. Avbildning av DABGRAF systemet, siste versjon som viser størrelsesmålinger av makrell i tett lag fra 70 -90 meters dyp, svinger rettet nedover.

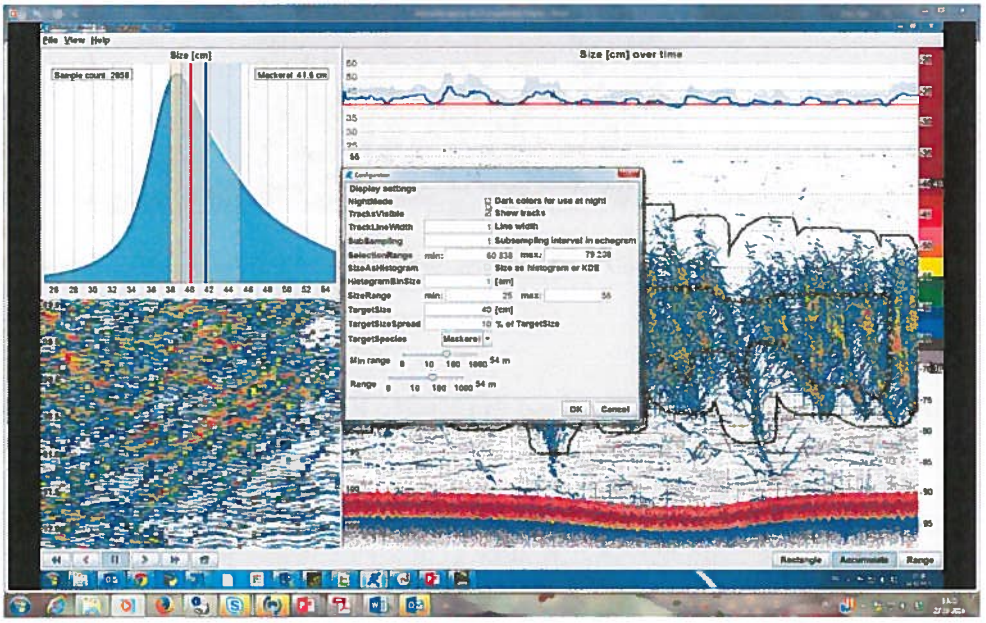

Figur 18. Avbildning av DABGRAF systemet, siste versjon som viser størrelsesmålinger av makrell i tett lag fra 70 -90 meters dyp, annen setting med visning av valgmuligheter av art, ønsket størrelse og andre nøkkeparametere.

Oppsummering, avvik og konklusjoner

Oppsummering

1. DABGRAF prosjektet har levert ny metodikk for størrelsesmåling av fisk med helt ny teknologi, bredbåndsekkolodd og smalstråle svinger
2. DABGRAF prosjektet har utviklet en fysikkbasert tilnærming til størrelsesmåling basert på kjente måleparametre for enkeltindivider som baserer seg på
    a. Oppløsning av enkle mål i kanten av stimen og i lag av fisk
    b. Målfølging av enkeltindivid (target tracking)
    c. Beregning av ekkostyrke (TS) i frekvensområdet 170-270 kHz
    d. Spekteranalyse og beregning av null-punkts-differanser
    e. Beregning av puls strekking av signalet
3. CMR har i samarbeid med Havforskningsinstituttet utviklet programvare for direkte lesing av de store datamengdene som kommer fra EK80 i bredbånds, FM modus, 170-270 kHz, og implementert sanntids beregning av fiskestørrelse basert på data fra pkt. 2.
4. Videre er det utviklet et visuelt grensesnitt, der en kan visualisere ekkogrammene, data-deteksjon og størrelsesfordeling på skjerm.
5. HI har utviklet metoder for kalibrering av bredbånds ekkolodd i samarbeid med Simrad
6. HI og CMR har presentert DABGRAF og størrelsesmålingsmetoden nasjonalt og internasjonalt på møter og konferanser. Metoden er ennå ikke skikkelig publisert internasjonalt, men dette har vi rimelig tid til fordi vi er de eneste i verden som har et slikt høyoppløsnings-system i dag.

Avvik:

1. Det har oppstått en del avvik med hensyn på målinger og rapportering fordi ferdig versjon av prototype ekkolodd og dataformater kom senere enn forventet, og dataopptak måtte utsettes 1 år og 2 år fordi CRISP /DABGRAF toktene har gått om høsten.
2. I det opprinnelige DABGRAF prosjektet ville en bruke modellbasert ekkomodell for sild og makrell, men det viste seg at denne gav ustabile resultater. For å rette på dette måtte en utføre direkte, eksperimentelle målinger i Austevoll med måling av fiskens direktivitet i lateral aspekt. Målerigg og målinger / bearbeiding av dette materialet tok lang tid, og var av økonomiske hensyn begrenset til fiskestørrelser som fantes i levendelagring i Austevoll. Ideelt skulle lengdespredningen både for sild og makrell vert større.
3. Systemet har ikke blitt brukt til skikkelig validering enda, delvis på grunn av manglende data på ulike lengdegrupper av sild og makrell, men mest fordi prosjektet er egentlig formelt avsluttet. Videre valideringer må foregå under CRISP tokt, der et av delmålene er størrelse måling av fisk, men med mindre innsats enn når DABGRAF prosjektet var aktivt.

Konklusjoner

1. DABGRAF prosjektet har utviklet levert et system for akustisk størrelsesmåling av fisk med programvare for visning og evaluering.
2. Validering av størrelsesmålingens nøyaktighet må gjennomføres av andre prosjekter eller i et nytt prosjekt, gjerne der størrelsesmålingen blir utført fra fiskefartøy.
3. Ny svingermontering for fiskefartøy, der svingeren kan roteres ut fra normal vertikal ut til horisontal, må utvikles og utprøves. Motoriseringen av svingeren bør kunne følge sonar-tilt.
4. Metoden og programvaren er ennå meget aktuell både for norske fiskere og for utenlandske fiskere i tilsvarende fiske.

REFERANSER

1. Brede, R., Kristensen, F. H., Solli, H., & Ona, E. (1990). Target tracking with a split-beam echo sounder. *Rapp PV Reùn Cons Int Explor Mer*, *189*, 254-263.

2. Chu, D., & Stanton, T. K. (1998). Application of pulse compression techniques to broadband acoustic scattering by live individual zooplankton. *The Journal of the Acoustical Society of America*, *104*(1), 39-55.

3. Godø, Olav Rune, et al. "Detecting Atlantic herring by parametric sonar." *The Journal of the Acoustical Society of America* 127.4 (2010): EL153-EL159.

4. Handegard, N. O., Patel, R., and Hjellvik, V. (2005). "Tracking individual fish from a moving platform using a split-beam transducer," J. Acoust. Soc. Am. **118**, 2210–2223.

5. Handegard, N. O. (2007). Observing individual fish behavior in fish aggregations: Tracking in dense fish aggregations using a split-beam echosounder. *The Journal of the Acoustical Society of America*, *122*(1), 177-187.

6. IMR Cruise reports : 2012116, 2013003, 2013115, 2014119

7. Macaulay, G., Ona, E., Andersen, L.N., Korneliussen, R., and Calise, L. 2012. Calibration of a broadband split-beam echo sounder and broadband spectra from selected targets. ICES FAST WG 2012.

8. Macaulay, G. J., Peña, H., Fässler, S. M. M., Pedersen, G., & Ona, E. (2013). Accuracy of the Kirchhoff-Approximation and Kirchhoff-Ray-Mode Fish Swimbladder Acoustic Scattering Models. *PLoS ONE*, *8*(5), e64055. http://doi.org/10.1371/journal.pone.0064055

9. Ona, E. 1990. Physiological factors causing natural variations in acoustic target strength of fish. J. Mar. Biol. Ass. U.K. (1990), 70, 107-127.

10. Ona, E. (1999). Methodology for target strength measurements (with special reference to in situ techniques for fish and micro-nekton) No. 235. *ICES Cooperative research report* 235, 1999.

11. Ona, E, et al. "Exploratory measurements using a broadband, split beam echo sounder system." *The Journal of the Acoustical Society of America* 129.4 (2011): 2696-2696.

12. Pobitzer, A., Ona, E., Macaulay, G., Korneliussen, R., Totland, A., Heggelund, Y., Eliassen, I.K. 2015. Pre-catch sizing of herring and mackerel using broadband acoustics. ICES Symposium on "Marine Ecosystem Acoustics (Some Acoustics)–observing the ocean interior in support of integrated management". Nantes, France, from 25 May 2015 to 28 May 2015.

13. Sawada, K., Furusawa, M and Williamson, M.N. (1993) Conditions for the precise measurement of fish target strength in situ. J. Mar. Acoust. Soc.. Jpn., 20 (1993), pp. 73–79

14. Simmonds, E. J., and MacLennan, D.N. 2005. **Fisheries Acoustics: Theory and Practice**. Ames, Iowa: Blackwell Science, Oxford (2005)

15. Stanton, T. K., Reeder, D. B., & Jech, J. M. (2003). Inferring fish orientation from broadband-acoustic echoes. *ICES Journal of Marine Science: Journal du Conseil*, *60*(3), 524-531.

16. Stanton, T. K., Chu, D., Jech, J. M., and Irish, J. D. 2010. "New broadband methods for resonance classification and high-resolution imagery of fish with swimbladders using a modified commercial broadband echosounder." *ICES Journal of Marine Science: Journal du Conseil* 67.2 (2010): 365-378.

17. Løvik, A., and Hovem, J. M. 1979. An experimental investigation of swimbladder resonance in fishes. Journal of the Acoustical Society of America, 66: 850–854.

APPENDIX I

Handegard 2007: Target tracking
Stanton et al (2003)

Observing individual fish behavior in fish aggregations: Tracking in dense fish aggregations using a split-beam echosounder

Nils Olav Handegard and KGF

Citation: J. Acoust. Soc. Am. **122**, 177 (2007); doi: 10.1121/1.2739421
View online: http://dx.doi.org/10.1121/1.2739421
View Table of Contents: http://asa.scitation.org/toc/jas/122/1
Published by the Acoustical Society of America

Observing individual fish behavior in fish aggregations: Tracking in dense fish aggregations using a split-beam echosounder

Nils Olav Handegard[a)]
Institute of Marine Research, Bergen, Norway

(Received 2 May 2006; revised 5 April 2007; accepted 21 April 2007)

Acoustic instruments are important tools for observing the behavior of aquatic organisms. This paper presents a simple but efficient method for improving the tracking of closely spaced targets using a split-beam echosounder. The traditional method has been a stepwise approach from the detection of echoes, rejection of apparently multiple targets and then tracking the remainder. This is inefficient because the split-beam angles are not included in the initial detection; rather they are only used in the rejection criteria before the subsequent tracking. A simple track-before-detection method is presented, where the phase angles, echo intensities, ranges, and times are used simultaneously, resulting in better detection and tracking of the individual fish. Two test data sets were analyzed to determine the effectiveness of this method at discriminating individual tracks from within dense fish aggregations. The first data set was collected by lowering a split-beam transducer into a herring layer. The second data set, also collected with a split-beam transducer, was from a caged aggregation of feeding herring larvae. Results indicate the potential of target tracking, using a split-beam echosounder, as a tool for understanding interindividual behavior. © *2007 Acoustical Society of America.* [DOI: 10.1121/1.2739421]

PACS number(s): 43.30.Sf [KGF] Pages: 177–187

I. INTRODUCTION

Ecosystem studies depend on knowledge of the individual components. Several studies have shown the feasibility of using various acoustic methods for measuring the behavior of individual targets *in situ*, both for fish (Arrhenius *et al.*, 2000; Torgersen and Kaartvedt, 2001) and plankton (Jaffe *et al.*, 1999; Klevjer and Kaartvedt, 2003). A particularly nice example is Genin *et al.* (2005), where the observed swimming behavior of zooplankton relative to water currents has been used to explain the observed aggregation patterns. Among other acoustical studies concerning the behavior of individuals are the behavior of over-wintering herring in the Ofotfjord (Huse and Ona, 1996), vertical search patterns in fish (Cech and Kubecka, 2002), diel differences in swimming patterns in fish (Gjelland *et al.*, 2004) and zoo-plankton (De Robertis *et al.*, 2003), behavioral changes induced by a trawling vessel (Handegard *et al.*, 2003; Handegard and Tjøstheim, 2005), and the feasibility for devices to prevent fish entering hydroelectric turbine intake (McKinstry *et al.*, 2005). McQuinn and Winger (2003) used manual tracking to investigate the impact of diel-dependent fish behavior on target strength. Riverine and shallow-water research is another large field where acoustic methods have been used to observe fish behavior, with special emphasis on migratory behavior and counting (Enzenhofer *et al.*, 1998; Mulligan and Chen, 1998; Mulligan and Kieser, 1996). This interest is motivated by the fact that echo integration is difficult to apply in a riverine environment.

Schooling behavior is a spectacular pattern in nature, and there have been many attempts to uncover the dynamics of this phenomenon. Parr (1927) introduced the idea of simple repulsive and attractive "forces" between individuals, and these ideas were further developed by Breder (1954) and Sakai (1973). The first individual-based data simulation was reported by Aoki (1982). Similar model approaches have been described by Reynolds (1987) and Huth and Wissel (1992). All these models demonstrate that simple rules on the individual can result in complex school dynamics. However, data to support these models are scarce, and methods capable of quantifying interindividual behavior are needed, in particular for closely spaced individuals. The latter problem is the main motivation for the present study, but the method is general and is also useful for other tasks involving the detection of single individuals, e.g., target strength measurements. The goal of this work, therefore, is to develop an improved method for tracking closely spaced individual targets using split-beam echosounders.

A. The state of the art

Two different acoustic instruments for observing behavior are the multibeam sonar, see, e.g., Jaffe *et al.* (1995), and the split-beam echosounder (Brede *et al.*, 1990; Ehrenberg and Torkelson, 1996). The multibeam sonar can handle several targets at a given range, but the resolution is limited by the number of beams and their opening angles. There are, however, methods to compensate for this problem (Jaffe, 1999; Schell and Jaffe, 2004), but at the cost of being able to observe fewer animals at the same range. The somewhat simpler split-beam echosounder is ineffective when multiple targets are located at the same range (Foote, 1996). The split-

[a)]Electronic mail: nils.olav.handegard@imr.no

7. Macaulay, G., Ona, E., Andersen, L.N., Korneliussen, R., and Calise, L. 2012. Calibration of a broadband split-beam echo sounder and broadband spectra from selected targets. ICES FAST WG 2012.

8. Macaulay, G. J., Peña, H., Fässler, S. M. M., Pedersen, G., & Ona, E. (2013). Accuracy of the Kirchhoff-Approximation and Kirchhoff-Ray-Mode Fish Swimbladder Acoustic Scattering Models. *PLoS ONE*, *8*(5), e64055. http://doi.org/10.1371/journal.pone.0064055

9. Ona, E. 1990. Physiological factors causing natural variations in acoustic target strength of fish. J. Mar. Biol. Ass. U.K. (1990), 70, 107-127.

10. Ona, E. (1999). Methodology for target strength measurements (with special reference to in situ techniques for fish and micro-nekton) No. 235. *ICES Cooperative research report* 235, 1999.

11. Ona, E, et al. "Exploratory measurements using a broadband, split beam echo sounder system." *The Journal of the Acoustical Society of America* 129.4 (2011): 2696-2696.

12. Pobitzer, A., Ona, E., Macaulay, G., Korneliussen, R., Totland, A., Heggelund, Y., Eliassen, I.K. 2015. Pre-catch sizing of herring and mackerel using broadband acoustics. ICES Symposium on "Marine Ecosystem Acoustics (Some Acoustics)–observing the ocean interior in support of integrated management". Nantes, France, from 25 May 2015 to 28 May 2015.

13. Sawada, K., Furusawa, M and Williamson, M.N. (1993) Conditions for the precise measurement of fish target strength in situ. J. Mar. Acoust. Soc.. Jpn., 20 (1993), pp. 73–79

14. Simmonds, E. J., and MacLennan, D.N. 2005. **Fisheries Acoustics: Theory and Practice**. Ames, Iowa: Blackwell Science, Oxford (2005)

15. Stanton, T. K., Reeder, D. B., & Jech, J. M. (2003). Inferring fish orientation from broadband-acoustic echoes. *ICES Journal of Marine Science: Journal du Conseil*, *60*(3), 524-531.

16. Stanton, T. K., Chu, D., Jech, J. M., and Irish, J. D. 2010. "New broadband methods for resonance classification and high-resolution imagery of fish with swimbladders using a modified commercial broadband echosounder." *ICES Journal of Marine Science: Journal du Conseil* 67.2 (2010): 365-378.

17. Løvik, A., and Hovem, J. M. 1979. An experimental investigation of swimbladder resonance in fishes. Journal of the Acoustical Society of America, 66: 850–854.

APPENDIX I

Handegard 2007: Target tracking
Stanton et al (2003)

beam echosounder does not depend on the grid-cell volume in the same way as the multibeam sonar, but it needs a fair signal-to-noise ratio to work properly (Kieser *et al.*, 2000). Both methods have limitations when observing dense aggregations of targets. This study focuses on the use of split-beam echosounders because of their relative simplicity and availability to researchers.

The split-beam echosounder transmits an echo pulse into the water column, and the backscattered signal is received on four quadrants of the transducer face. The phase differences between the four quadrants are used to estimate the direction to the target, so each sample (or pixel in the echogram) is associated with an intensity and two angles, in addition to the receive time and corresponding range as given by the location in the echogram. If there is a single target at a given range, the angles are representative of the position of that target. However, if there is no target or there are multiple targets at the same range, the angles do not represent the position of a single target. It is thus not possible for two fish at the same range to provide valid observations.

Traditionally, obtaining target tracks from acoustic data has been a two-step process (Ehrenberg and Torkelson, 1996, p. 329). First, the targets are detected with a single-echo-detection (SED) algorithm, and then these detections are combined into tracks making use of their positions in successive pings. The potential of this method for observing fish behavior has been acknowledged for a long time (Foote *et al.*, 1986, 1984; Ona, 1994). In general, target tracking is a well-established field, see, e.g., Blackman and Popoli (1999), and has been further developed for split-beam data (Handegard *et al.*, 2005; Xie, 2000).

The SED targets were originally used to estimate the target strength (TS) of the individual fish within the echo beam (Brede *et al.*, 1990; Foote *et al.*, 1986, 1984; Ona, 1999). For this purpose, it is crucial to avoid two targets being considered as one since this would positively bias the results (Foote, 1996). Different methods to reject SED targets contaminated with multiple targets include the use of phase, amplitude, and echo-duration information from the returned echo, see Soule *et al.* (1996) for an evaluation of these methods. When successful, the results of SED algorithms are high-quality targets with corresponding estimates of TS and location in the beam. However, the SED algorithms are not designed for tracking purposes, and there are often missing pings within a track due to the strict SED rejection criteria. The SED algorithm works on ping-by-ping data, and little effort has been applied to use the temporal dimension of the data to improve single-echo detection. One exception is Balk and Lindem (2000), who use the information in adjacent samples (range and time) to decide whether a sample in the echogram belongs to a target or not, a technique known as cross-filter detection which is used to aid the SED algorithm. This, along with other tracking tools, is implemented in the SONAR 5 software (SONAR 5 user manual, Helge Balk, University of Oslo, Norway). The idea of using the temporal dimension is intellectually appealing, since it utilizes information that "conventional" detectors discard. The SONAR 5 software can also interpolate sample data between already-detected SED targets, leading to better tracking performance than conventional methods.

B. Posttracking detection

In this paper, the target angles, echo intensity, time, range, and the actual tracking results are considered in one single step. It is not based on the traditional stepwise process of detection, rejection, and tracking, where the angles are used as rejection criteria only, and single targets must be passed by the SED algorithm to initiate tracks. The idea is inspired by the track-before-detect approach (Blackman and Popoli, 1999, p. 18). In order to achieve this, all samples above a threshold are initially treated as single targets. Note that a target is typically composed of several samples. The threshold is set lower than the expected intensity of the target echoes, ensuring that no targets are lost. Consequently, low intensity samples where no fish are present are treated as valid targets. Each sample has its own apparent position and intensity. The range and time are determined by the sample (pixel) position in the echogram, while the angles and intensities are given by the pixel values in the echogram and "anglegrams,"[1] respectively. The low threshold results initially in many false targets, but the advantage is that no information is lost in this initial step, as opposed to the traditional approach, where the SED algorithm rejects many targets. This calls for a different approach when associating samples to tracks, by postponing the quality screening until the tracks have been established, which may be denoted "track rejection" as opposed to the single-target rejection applied in the SED algorithm. The main objective of this paper is to develop these techniques.

II. MATERIALS AND METHOD

This section is divided into three main parts. First the test data sets are presented. The second part is the actual method of data association, i.e., associating samples to tracks. Finally the track rejection and track quality algorithms are described. The other aspects of the tracking, like track estimation, incorporating platform movement, etc., are the same as described in Handegard *et al.* (2005). That paper is somewhat technical, and it is not necessary to fully understand the details there to appreciate the ideas presented here. However, track estimation is an important part of any tracking system, and therefore a paragraph in Sec. IV briefly addresses these questions.

A. Test data

Test data set I [see Figs. 1(a)–1(d)] was obtained by a Simrad EK60 split-beam echosounder with a Simrad 38DD, a 38-kHz, 7°-beamwidth circular transducer. This transducer is depth stabilized and certified to be used down to 1500 m depth. The test set is taken looking horizontally into a herring (*Clupea harengus*) layer. The reason for aligning the sounder horizontally was originally to investigate the horizontal-aspect TS for herring, but it is also the preferred orientation when observing interindividual fish behavior, since there are indications that the fish will orientate relative to the neighboring fish horizontally more so than vertically

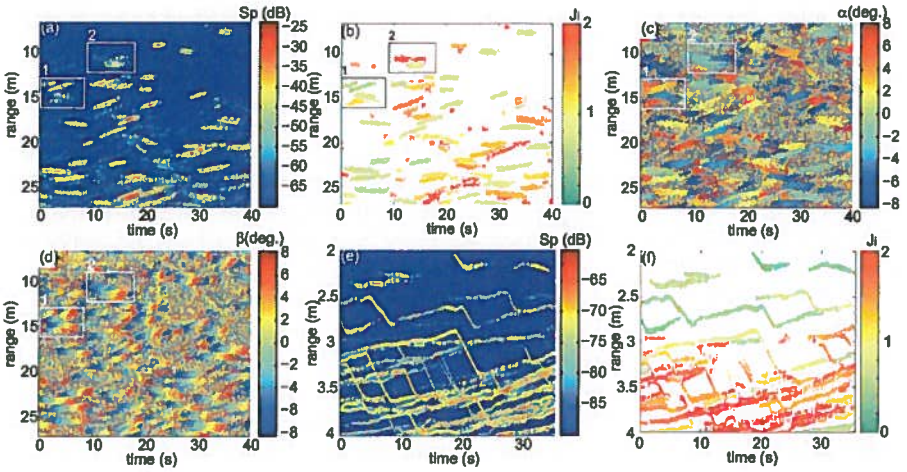

FIG. 1. (a) The example echogram for data set I. The echogram is given in S_p (dB re m^2) units. The boxes labeled 1 and 2 are the subsets 1 and 2, which are used as examples of successful and unsuccessful tracking, see Figs. 4 and 5, respectively. (b) The track quality for each track, J_i, where red indicates rejected tracks ($J_i > 1$) and green indicates accepted tracks ($J_i \leq 1$). Tracks with $J_i > 2$ are shown as $J_i = 2$. (c), (d) The corresponding alongship and athwart ship angles, respectively, in degrees. (e) The echogram for data set II and (f) the resulting quality of the tracks in test data set II, J_i.

(Grünbaum)[2]. The range of the probing echosounder was set to 27 m allowing for a very high ping rate of 17 Hz. In addition the sample interval was set to 9.4 cm with a pulse duration time τ of 512 μs. The output power P_t was set to 200 W. All data recorded closer than 6 m were discarded due to near field effects. The received power was converted to $S_p = 10\log(s_p)$ with unit dB re m^2, where

$$s_p = \frac{P_{r,i} 16\pi^2}{P_t g_0^2 \lambda^2} r_i^4 10^{2\alpha r_i}.$$

Here P_t is the output power, g_0 is the on axis gain, λ is the wavelength, α is the absorption coefficient, $P_{r,i}$ is the received power in sample i, and r_i is the corresponding range. In fisheries acoustic terms, this corresponds to time varied gain (TVG) of 40 log r and no beam pattern compensation.

Test data set II [see Figs. 1(e) and 1(f)] was obtained by a Simrad EK60 Split-beam echosounder with a Simrad ES 200-7C, a 200-kHz, 7°-beamwidth circular transducer, looking vertically into a cylindrical container of black polyethylene sheeting. The aim of this experiment was to investigate feeding behavior of herring larvae in a wide and physically controlled volume of sea water (a mesocosm). The bag was supported by ropes attached to a stainless steel circular ring connected to an open raft in a sheltered bay. The bag and the raft constituted a single entity floating on the sea surface. The pulse duration time τ was 64 μs, with a corresponding sample interval of 1.2 cm, and a ping rate of 16.8 Hz. The output power P_t was set to 1000 W.

In order to compare the present method to the original SED algorithm, single targets are detected in test data set I by the SED algorithm incorporated in the EK60 and by the SONAR 5 software. The echo-length acceptance criteria are set wide and the phase deviations high in order to reject less targets (Table I).

B. The method

Since the sample data are being used directly, no prior detection is necessary. The idea is that samples are treated as targets and that several samples from the same ping may be associated with the same single target, somewhat similar to the concept of joint probabilistic data association (Blackman and Popoli, 1999, pp. 353–355), but probabilities of detection are not considered and multiple samples may not be shared by two tracks.

A tracking system consists of several steps, including track estimation, track prediction, gating, data association, and track support. Gating, data association, and track support are presented in detail in the following, but track estimation and track prediction are only summarized. The details are presented in Handegard *et al.* (2005).

Prior to tracking, a threshold is set to initially remove samples not being targets. This threshold is set low to ensure that weak targets are not missed in the subsequent algorithm. The thresholds for data sets I and II are −70 and −90 dB, respectively, and are set based on visual inspection of the echograms [Figs. 1(a) and 1(e)] with different thresholds.

Each sample above the threshold is treated as an observation, and consists of $\mathbf{y} = [\alpha\ \beta\ r\ I]$, where α and β are the alongship and athwartship angles, respectively, r is the range, and I is the energy of the sample. The intensity measure used here is S_p.

TABLE I. The EK60 and SONAR 5 single-echo-detection (SED) settings for the case I test set. The parameters are chosen to allow more detections than the typical settings. The "echo lengths" are given as a factor multiplied with the pulse duration time τ. Maximum phase deviation is the maximum allowed average electrical phase jitter between samples inside an echo from a single target. For the echosounder and transducer used here (case I), one phase step corresponds to 0.064°. The recommended setting for weak targets is four to ten phase steps. Maximum gain compensation is the correction value from the one-way model of the transducer beam pattern. For the Simrad 38DD transducer, this corresponds to a maximum acceptable off-axis angle of ~5°. The threshold is applied to the echogram in S_p (dB re m^2) units.

	EK60	SONAR 5
Software version	1.4.4.66	v5.9.6
Minumum echo length (s)	0.2τ	0.2τ
Maximum echo length (s)	2.7τ	2.7τ
Maximum phase deviation (phase steps)	10.0	23.0
Maximum gain compensation (dB)	6.0	6.0
Threshold (dB)	−50	−50
Multiple peak suppression	N/A	Off
Min distance between detections (cm)	N/A	1

TABLE II. The tracking parameters for data set I and data set II: The threshold (TH), the gate parameters (α_g, β_g, r_g, and I_g), the track initiation parameters (α_0, β_0, r_0, I_0, and N_0), the track termination parameters, including the maximum within gate conflicts (N_c), the maximum number of missing samples between the first and last sample in range (N_e), the maximum number of successive missing pings (N_m), and the track rejection parameters, including the missing pings to track-length ratio (NM), the track length (TL), and the samples to track length ratio (NL).

	TH (dB)	α_G β_G (deg)	r_G (m)	I_G (dB)	α_0 β_0 (deg)	r_0 (m)	I_0 (dB)	N_0	N_c	N_e	N_m	MN	TL	NL
Data set I	−70	2.80	0.44	20	2.80	0.12	20	5	3	2	1	0.80	8	2.00
Data set II	−90	1.80	0.10	20	2.00	0.03	20	5	2	2	1	0.80	8	2.00

At each time step, the track state $\mathbf{x}$ (position, velocity, and echo intensity) for each live track is estimated using a Kalman filter, and assuming constant velocity, the state is predicted at the next time step [Handegard *et al.*, 2005, their Eq. (5)]. The predicted state is denoted $\tilde{\mathbf{x}}$.

To compare predictions with observations, the predicted state $\tilde{\mathbf{x}}$ is mapped to observation space, i.e., $\tilde{\mathbf{x}} \rightarrow \tilde{\mathbf{y}}$. For the position, this involves mapping the Cartesian position of the track to alongship angle, athwartship angle, and range [Handegard *et al.*, 2005, their Eq. (4)]. The velocity is not part of the mapping, and the echo intensity is the same in both spaces. This allows us to define a distance metric between a sample $\mathbf{y}$ and a live track $\tilde{\mathbf{y}}$ (predicted position in observation space). The metric is the so-called gate distance defined in the following.

1. Gating

The first part of the data association is the gating. This decides which samples should be considered to be parts of the track. In the following, i, j, and k denote track number, sample number, and ping number, respectively. The difference between the prediction from track i and sample j is calculated for all predictions and samples at ping k, i.e.,

$$\hat{\boldsymbol{\epsilon}}_{ijk} = \mathbf{y}_{jk} - \tilde{\mathbf{y}}_{ik}. \tag{1}$$

The gate distance

$$d_{ijk} = \hat{\boldsymbol{\epsilon}}_{ijk} G \hat{\boldsymbol{\epsilon}}_{ijk}^{T} \tag{2}$$

is a measure of closeness between samples and predictions. If $d_{ijk} \leq 1$, sample j is inside the gate of track i at ping k. Here T is matrix transpose and

$$G = \begin{bmatrix} \alpha_G^2 & 0 & 0 & 0 \\ 0 & \beta_G^2 & 0 & 0 \\ 0 & 0 & r_G^2 & 0 \\ 0 & 0 & 0 & I_G^2 \end{bmatrix}^{-1}. \tag{3}$$

Note that the intensity is also included in the gate. The elements in G are set as parameters in this case, α_G, β_G, r_G, and I_G being the maximum allowed deviances between the observation and the prediction along each dimension (see Table II). This means that if the maximum deviation occurs in α, no deviance is allowed in any of the other dimensions. Consequently, the maximum deviance rarely occurs. The interpretation is that the observation must be within a hyperellipsoid defined by $d \leq 1$ (see Fig. 2). There are ways to set the gate parameters based on detection probabilities and innovation covariances, i.e., the covariance of $\hat{\boldsymbol{\epsilon}}$, but this is not done here, cf. the discussion to follow.

2. Data association

The next step is to associate the samples inside the gates to tracks. At each ping a gate is calculated for each live track, but a given sample may be inside more than one gate, and a given gate may contain more than one sample. If there are no conflicts, i.e., no samples lie within more than one gate, each sample is associated to the corresponding track. If there are conflicting observations, they are associated to the "closest" track in terms of d. However, if the number of conflicting observations inside a gate is higher than the *ad hoc* parameter N_c, the shortest track is automatically terminated. In general the N_c parameter is a crude method to avoid wrong associations, and tuning the gates are preferred over decreasing N_c. The result of the data association step is that each sample j at ping k that are deemed part of a track i is associated with track number i. The set of samples j associated with track i at ping k is denoted A_{ik}. Similarly, the set A_i is defined as the set of all samples associated with track i over the full duration of the track.

The observations j that are associated to track i at ping k are then combined into a composite observation by

$$\mathbf{y}'_{ik} = \frac{\sum_{j \in A_{ik}} w_{ijk} \mathbf{y}_{jk}}{\sum_{j \in A_{ik}} w_{ijk}}, \tag{4}$$

where $w_{ijk} = \exp(-d_{ijk}^2)$. This weighted observation is used in the Kalman update equation. This approach is analogous to joint probabilistic data association, where the weights are

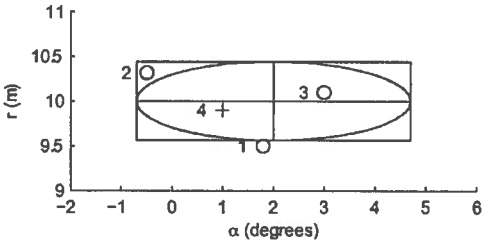

FIG. 2. Two-dimensional projection of the four-dimensional gating process; the center of the ellipsoid is the prediction by the Kalman filter algorithm. Four samples are given for illustrative purposes. Sample 1 is outside the range gate r_G, sample 2 is inside the range of r_G and α_G separately (illustrated by the rectangle), but outside the ellipsoidal gate since the deviations are summed. Sample 3 is inside the gate of r_G and α_G (illustrated by the ellipse), but the gate is four dimensional, and this sample lies outside the ellipsoidal gate, because of a large offset in β. Finally, sample 4 lies within the ellipsoidal gate and is associated with the prediction.

determined by closeness to the prediction, but detection probabilities are not considered here. The updated state variables are used to obtain predictions for the next time step, and then the process is repeated.

3. Initiating and terminating tracks

Before proceeding to the next time step, samples not associated with tracks are used as candidates for new tracks. Initiating new tracks is difficult since there are usually several sample values for each new target. The method chosen for initiating new tracks is similar to the tracking of already established tracks. The nonassociated samples within a ping are compared in pairs (each sample is paired with the next adjacent sample). By taking the first sample as a prediction and the second as an observation, Eqs. (1) and (2) can be used to calculate the distance between them, using the track-initiation gate

$$G_0 = \begin{bmatrix} \alpha_0^2 & 0 & 0 & 0 \\ 0 & \beta_0^2 & 0 & 0 \\ 0 & 0 & r_0^2 & 0 \\ 0 & 0 & 0 & l_0^2 \end{bmatrix}^{-1} \tag{5}$$

instead of the regular gate. If the difference between these samples is less than unity, i.e., the second is within the gate of the first, the second sample is compared with the next adjacent sample is range, etc., forming a chain of samples that are within each other's gates. When a sample does not fall within the gate of the previous, the chain is determined. If the length of the chain is larger than N_0, a new track is formed based on the mean of these samples. If many adjacent samples (in range) meet the criteria, there is a possibility for combining several new targets into one, and this will occasionally happen. Several tools have been developed to remove or to flag these tracks as low-quality results, cf. Sec. II C.

Track termination is the method applied to close a track during tracking. Three methods for track termination are implemented. The gate-conflict parameter N_c has already been defined as the maximum number of conflicting targets within a gate. Furthermore, when tracking very weak targets, the background reverberation may be tracked. These "tracks," however, typically have several missing samples within them. To terminate these tracks, the number of missing samples between the first and last sample (in range) are counted, and if they exceed N_e samples, the track is terminated. Finally, the number of successive missing pings, N_m, is used. However, after a track is terminated, other techniques can be used to test its quality or to reject it, cf. Sec. II C.

C. Quality control

When tracking fish in dense registrations, misassociations and track-split errors will inevitably occur, and a method to reject or to flag each track with an association-quality measure is important. The track quality algorithm is based on measures of association errors, and the track rejection algorithms are based on more *ad hoc* criteria. The criteria adopted for rejecting tracks are simply the number of missing pings to the track length ratio (MN) the track length (TL), and the total number of samples to the track length ratio (NL). These are set as parameters.

Previously, association errors have been investigated for single targets, i.e., false or missing associations between single detections (Handegard *et al.*, 2005, see, e.g., their Sec. III D). However, that measure cannot be used here because target detection and tracking are not separated. Since the algorithm presented here works on samples, misassociation in range may also occur, both as connection errors (one track may consist of several fish) and track-split errors (several adjacent tracks may be formed from one single fish). Four measures of track quality have been defined. The first two measures take a global approach where no particular misassociation type is addressed, whereas the two last measures deal with track connection and track-split errors in range, respectively.

One way to investigate association errors is to compare the results from a forward and backward run through the data set. If questionable associations have occurred, it is likely that a different result would be obtained by running the data association backwards, i.e., starting from the end of the data set and progressing to the beginning. For a given track in the primary data set, e.g., the forward run, the samples associated with track i are given by A_i. Let B_l be the set of samples associated with track l from the backward run. The intersection is given by $A_i \cap B_l$, and let N_{A_i}, N_{B_l}, $N_{A_i \cap B_l}$ be the number of samples in the respective sets. Two measures comparing the backward and forward runs are defined. Let

$$J_{a,i} = 1 - \max_l (N_{A_i \cap B_l}) / N_{A_i}. \tag{6}$$

This results in a measure of how well the "best" backward track overlaps the forward track, and the identifier l for that track. The range of J_a is [0 1], where a high value indicates that the forward track contains false associations or the backward track is split. Let

$$J_{b,i} = 1 - (N_{A_i \cap B_l}) / N_{B_l}, \tag{7}$$

where l is the backward track that maximized $N_{A_i \cap B_l}$ in Eq. (6). Again the range is [0 1], and a high J_b value indicates the occurrence of track-split errors in the forward track or false association in the backward track. Since the index l is taken from Eq. (6), J_a do not necessarily become J_b when using the backward run as the forward run. This procedure is illustrated in Sec. III on a subsample of the test data set I, cf. Fig. 5.

The track initialization algorithm may be stricter than that used to continue an already initiated track; one result of this could be a late initiation of tracks. By combining high-quality-forward and backward tracks in terms of J_a and J_b, the dependence on track initiation parameters may be reduced. The new track is defined by the union $A_i \cup B_l$ of the matched tracks. If weak targets along the edges of the tracks are a concern, the intersection between the forward and backward track, $A_i \cap B_l$, can be used instead.

A track-split error may occur if the tracks are initiated incorrectly, i.e., when two tracks are initiated for one fish, or

if the gates from two tracks cover the same samples. This can be observed in the echogram as two adjacent tracks, where the tracks are not separated by any nonassociated samples. A measure to detect this effect is simply to check the sample above and below the track. If that sample belongs to another track, a track-split error may have occurred, i.e.,

$$J_{\text{split},ik} = \frac{N_a}{2}, \tag{8}$$

where $N_a \in \{0,1,2\}$ if there is, or not, an adjacent track above, below, or both at ping k for track i. The factor $1/2$ is for scaling the measure to the range [0 1]. For the whole track

$$J_{\text{split},i} = \frac{1}{L_i}\sum_{k}^{L_i} J_{\text{split},ik}, \tag{9}$$

where L_i is the length of the track (excluding missing pings).

A track merging error in range occurs when one track is formed from two fish, e.g., if the initiation and tracking gates are set too wide. It is desirable to set the gates wide to capture rapid changes in behavior, but at the possible cost of misassociation, both in range and time. However, using standard SED rejection criteria, misassociations in range can be monitored. Following the recommendations of Soule *et al.* (1996) for successful multiple-target rejection in SED algorithms, the phase angle deviation over one target in one ping is calculated as a measure of track-combination error in range, i.e.,

$$J_{\text{merge},ik} = \frac{1}{2}\left[\frac{1}{N_{A_{ik}}-1}\sum_{j\in A_{ik}}(\bar{\alpha}_{ik}-\alpha_{jk})^2\right]^{1/2} + \frac{1}{2}\left[\frac{1}{N_{A_{ik}}-1}\sum_{j\in A_{ik}}(\bar{\beta}_{ik}-\beta_{jk})^2\right]^{1/2}, \tag{10}$$

where $N_{A_{ik}}$ is the number of samples for track i at ping k and $\bar{\alpha}_{ik}$ and $\bar{\beta}_{ik}$ are the mean athwartship and alongship angles for track i and ping k, respectively. To use this measure for each track i,

$$J_{\text{merge},i} = \max_k (J_{\text{merge},ik}) \tag{11}$$

is defined. The maximum value is chosen since one erroneous association can severely bias the velocity estimate for the whole track. For applications where false associations are of less concern, the mean value could be used instead.

Four measures of quality control have been described. Each of these can be monitored individually, or they can be scaled relative to each other like

$$J_i = \left\{\left(\frac{J_{a,i}}{J_{a,0}}\right)^2 + \left(\frac{J_{b,i}}{J_{b,0}}\right)^2 + \left(\frac{J_{\text{merge},i}}{J_{\text{merge},0}}\right)^2 + \left(\frac{J_{\text{split},i}}{J_{\text{split},0}}\right)^2\right\}^{1/2} \leq 1, \tag{12}$$

where $J_{\text{merge},0}=1°$, $J_{\text{split},0}=0.3$, $J_{a,0}=0.3$, and $J_{b,0}=0.3$ are acceptable values for the different types of errors. This is, however, dependent on the application and is here implemented as changeable parameters.

Finally, the impact of various parameter settings on $J = (1/N)\Sigma_i^N J_i$, where N is the number of tracks, is investigated for both test data sets. The sensitivity measure is defined as

$$S_{pa} = 0.5\left(\frac{|\Delta J_{+10\%}|}{J} + \frac{|\Delta J_{-10\%}|}{J}\right)\left(\frac{|\Delta x|}{x}\right)^{-1}, \tag{13}$$

where $\Delta J_{+10\%}$ and $\Delta J_{-10\%}$ are the changes in J when perturbing parameter $pa \pm 10\%$, and $|\Delta x|/x = 0.1$, except for the parameters that are integers. To test the sensitivity to integer parameters, the parameter value is increased or decreased by one and $|\Delta x|/x = 1/N_0$, where N_0 is the unperturbed value. A similar method was used to test the sensitivity to data association in Handegard *et al.* [2005, their Eq. (15)].

III. RESULTS

The performance of the algorithm is demonstrated by its ability to associate samples in the test-data sets to tracks. First the results from the full data sets are presented (Fig. 1). Then subset 1 from data set I is used to demonstrate the ability to track closely spaced targets as compared to a traditional SED algorithm. Finally, subset 2 from data set I is presented as an example where the tracking fails. Here the importance of the track quality algorithm is shown.

The ability of the method to associate samples into individual tracks is presented in Figs. 1(b) and 1(f). The parameters for the association method are specified in Table II, and the general parameters used for the tracking, i.e., to obtain the prediction, etc., are similar to those in Handegard *et al.* (2005, their Table V, case I).

By inspecting the intensity echogram of test-data set I [Fig. 1(a)], distinctive tracks can be distinguished by eye. When simultaneously looking at the anglegrams [Figs. 1(c) and 1(d)], the tracks are more clearly separable. Actually, the angles are remarkably stable over a track, even if the echo intensity for the track is low. When visually comparing the echograms and anglegrams with the classification image [Fig. 1(b)], it is seen that the tracks are well detected. The distinctive tracks are classified as good tracks, whereas dubious registrations are marked as low-quality tracks. The same can be seen in the results for test-data set II [Fig. 1(e)].

The tracking algorithm can be used to separate background reverberation samples and track samples. Here, background reverberation is defined as the signal from a nontargeted scatterer. The empirical distribution for intensity and angles for both background reverberation and signal samples are presented [Figs. 3(a) and 3(b), respectively]. There is an overlap between the signal and background reverberation distributions in intensity. This may be caused by the failure to detect the beginning of some of the low-quality tracks, which are thus being classified as background reverberation. Similarly, some background reverberation samples will be falsely associated with tracks. This is defined as association errors, see the following. When looking at the angle distributions, a typical "circular" distribution is seen for the targets [Fig. 3(b)]. If the targets were uniformly distributed within the beam with r degrees opening angle, the probability density along one angle, e.g., α, times the number of

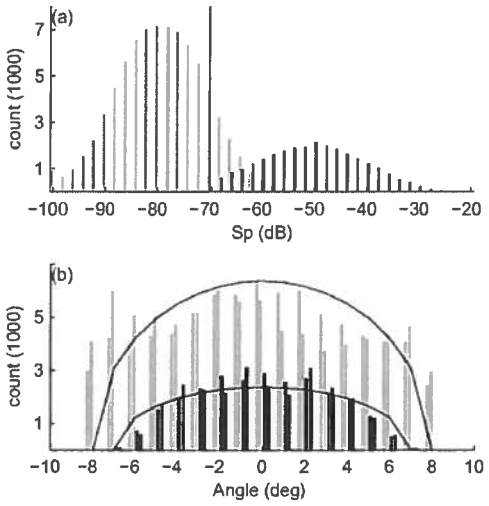

FIG. 3. The signal and background reverberation distributions. Signals are defined to be samples that belong to a track [see Fig. 1(b)], and background reverberation is defined to be samples more than two pixels away from a defined track. (a) The intensity distribution in S_p units (dB re m^2), where light gray bars are from background reverberation samples and black bars are from signal samples. The vertical line is the −70 dB threshold. (b) The angle distribution, where the light gray bars are background reverberation and black bars are signal. The first and second adjacent similarly colored bars are the alongship and athwart ship angles, respectively. The lines are the resulting angle distributions given uniformly distributed targets within $\alpha^2+\beta^2 \leq r^2$.

samples would be given by $y \sim N\sqrt{1-\alpha^2/r^2}/2\pi$, where N is the total number of samples. This seems to fit the results well, indicating that the targets ($r=7°$) were indeed randomly positioned across the beam. In the case of the background reverberation samples, the circular distribution is a less good fit (using $r=8°$). This distribution seems to be a combination of a uniform and a circular distribution. The uniform part is analogous to the model assumption in Kieser *et al.* [2000, their Eq. (4)]. The circular distribution component may originate from nondetected tracks or other nonfish scatters in the water column.

A subset of test-data set I, where closely spaced data are successfully tracked, is used to compare the ability of the tracker against the traditional SED, and to present the combination of forward and backward tracks (Fig. 4). The algorithm detects four tracks, but the EK60 SED does not accept many targets in this case. This may be beneficial when estimating TS, but is not necessarily an advantage for tracking purposes. SONAR 5 accepts more targets, but may also include more false targets. This is not so crucial, since the tracking algorithm would reject the false targets. However, both methods present several missing detections along a track. To illustrate the information used by the SED algorithm, the data contained in two separate pings are presented [See Figs. 4(d)–4(f) and Figs. 4(g)–4(i)]. To separate the targets, the conventional SED initially attempts to identify the peaks based only on the echo intensities. This may be possible in the first example [Fig. 4(f)] but is clearly not possible in the second example [Fig. 4(i)]. Success would also depend on the SED settings (Table I). If the threshold is set too low, several targets will be within the window and are thus rejected. However, when taking the angles into account, the tracks are separable. Tracks 20 and 24 are clearly separated by the alongship angles [Fig. 4(g)]. Without taking the angles into consideration, it would not be possible to properly track these signals. This is also demonstrated by the complete failure of both SED algorithms to detect track 20 [Fig. 4(a)]. The combination of forward and backward tracks are presented in Figs. 4(b) and 4(c). If the tracks meet the criteria of overlap i.e., $J_a<0.25$ and $J_b<0.25$ in this case, the forward and backward runs are combined into a single merged track. The tracks in this subsample meet the stated criteria, and are successfully merged [Fig. 4(b)]. Note that the track numbers are different in the forward and backward case.

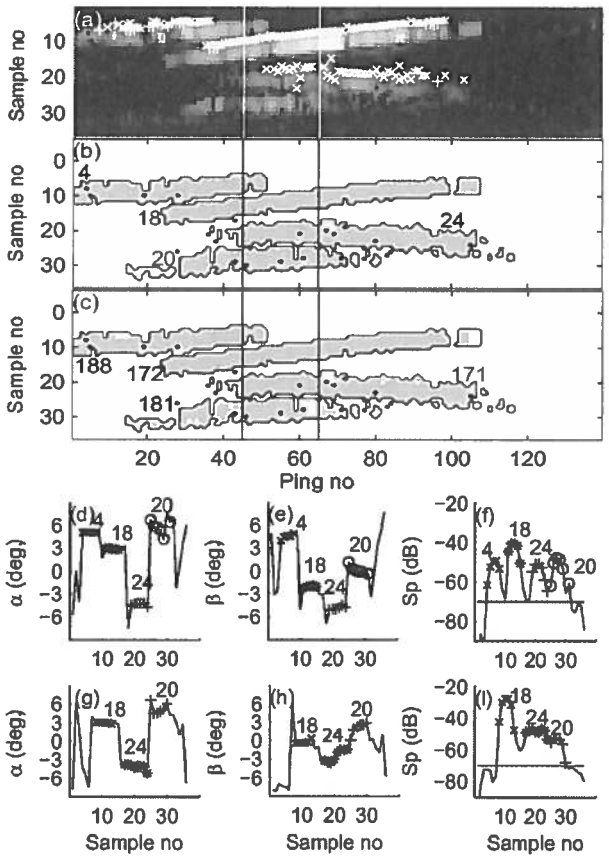

FIG. 4. Successful tracking of closely spaced targets. (a) The intensity echogram, where the white "+" and "×" denote the SED targets from EK60 and SONAR 5, respectively. The white vertical lines are the examples shown in (d)–(f) and (g)–(i), respectively. (b), (c) The forward and backward data association, respectively. Numbers indicate track numbers. The outlines denote the combination of the forward and backward tracking. Panels (d)–(f) and (g)–(i) show the intensity and angles for the samples indicated by vertical lines in (a)–(c). (×), (*), (+), and (○); Samples that have been associated with different tracks. The track numbers are printed above.

When the density is increasing, the limitations inherent in the split-beam principle will cause any tracking algorithm to fail. The track quality algorithm is thus an important part of the tracker, as it flags the cases where the tracker fails. Subset 2 of test data set I, where the algorithm fails, is used as an example (Fig. 5). Note that it is also difficult to determine tracks by visually inspecting the echogram and anglegrams [Figs. 1(a), 1(c), and 1(d), inside second box]. Since

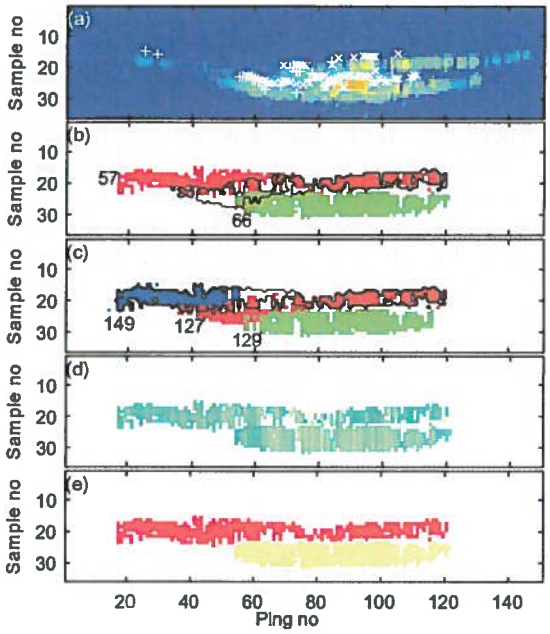

FIG. 5. Example of unsuccessful tracking. (a) The intensity echogram. The color scale is similar to Fig. 1(a). (b), (c) The results from the forward and backward tracking, respectively, on which J_a and J_b are based. Different colors indicate different tracks. Track 57 in the forward run (b) is taken as an example. The boundary from this track is transported to (c), i.e., the result from the backward run. It is seen that backward track 127 covers the largest proportion of this boundary, i.e., 46%. The J_a value is then $J_a=1-0.46=0.54$. Then the boundary of the backward track 127 is transported to the forward case panel (b). Track 57 covers 66% of this area, and thus $J_b=1-0.66=0.34$. (d) $J_{\text{merge},k}/J_{\text{merge},0}$ with the color-scale range from [0 2], similar to Figs. 1(b) and 1(f). (e) The resulting quality of the tracks, with the color scale range from [0 2], similar to (d).

the forward and backward tracking do not agree [Figs. 5(b) and 5(c)], and the merge and track-split errors are high (Table III), the algorithm marks the tracks as low quality. Further, the SED targets of the two algorithms are inconsistent in this case, and tracking these would yield doubtful results. The classification is done for both test-data sets [Figs. 1(b) and 1(f), Table III].

Sensitivity. The sensitivity test investigates the impact of

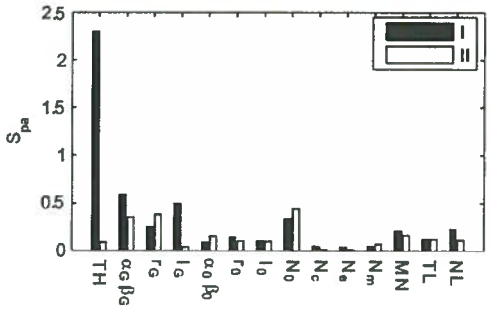

FIG. 6. The sensitivity S_{pa} for the different parameters, for data sets I and II, respectively.

parameter values on the track quality, giving an indication of which parameters are most important in the algorithm. The sensitivity for both test-data sets is given in Fig. 6. In general, the threshold, TH, is most important, followed by the gate and track initiation parameters. The lowest sensitivity is found in the track-termination parameters (N_c, N_e, and N_m). The sensitivity to the track-rejection parameters (MN, TL, and NL) is low, but this result depends on the initial parameter setting. If they are set to reject a large portion of the tracks, the rejection parameters become more important. Consequently, this test should be interpreted with care.

IV. DISCUSSION

The failure of the SED algorithm when tracking inside dense fish registrations was the motivation for this work, but there are other reports of problems with the SED procedure. Cronkite *et al.* (2004, their Sec. 4.3) discuss the problem of detecting closely spaced targets. They argue that the poor detection of closely spaced targets is caused by the echosounder SED algorithm, rather than acoustic shadowing within the aggregation. The inadequacy of the SED algorithm is thus not unique to the test cases reported here. In addition, the focus in fisheries acoustics has shifted from addressing technical problems like calibration, etc., to a more biological perspective, addressing behavioral considerations. This shift is evident in the Proceedings of the International

TABLE III. The first column indicates the test set I or II, and, where applicable, subset 1 or 2. The subsets refer to the boxes in Fig. 1(a), and Figs. 5 and 4, respectively. Where no track number is given, the mean of the respective data is presented, i.e., I,1 indicates the mean values from the tracks in subset 1 in test set I. I and II indicate the mean values of the full test sets. TrNoF and TrNoB indicate track numbers in the forward and backward cases, respectively, L_i is the track length (or mean length for the mean values) for the forward case, J_i (or J for the mean values), J_a, J_b, J_{merge}, and J_{split} are the quality measures defined in Sec. II C.

	TrNoF	TrNoB	L_i	J_i	J_a	J_b	J_{merge}	J_{split}
I,1	4	188	51	0.672	0.120	0.079	0.014	0.029
I,1	18	172	83	0.638	0.080	0.026	0.015	0.018
I,1	20	181	56	1.183	0.191	0.194	0.023	0.052
I,1	24	171	72	0.784	0.123	0.078	0.017	0.045
I,1			66	0.819	0.129	0.094	0.017	0.036
I,2	57	127	104	2.247	0.535	0.340	0.034	0.063
I,2	66	129	68	0.901	0.182	0.060	0.017	0.096
I,2			86	1.574	0.359	0.200	0.026	0.079
I			51	1.419	0.237	0.244	0.020	0.065
II			60	1.858	0.312	0.401	0.016	0.189

Council for Exploration of the Sea (www.ices.dk), which has sponsored symposia on fisheries acoustics (Craig, 1984; Karp, 1990; MacLennan *et al.*, 2003; Margetts, 1977; Massé *et al.*, 2003; Simmonds, 1996). Consequently, an improved methodology for addressing these questions is valuable.

Different applications make different demands on the tracking and detection algorithms. The SED algorithm was originally designed to estimate the TS of species of interest, and achieves this by rejecting low-quality targets (Soule *et al.*, 1996). By accepting only the high-quality-single targets, many pings may not register along the track in the subsequent tracking. This adversely results in split tracks and position errors, which in turn make the estimation of target velocity and position difficult. Apart from that, there are other problems with rejecting weak and low-quality targets before tracking. For example, estimates of target strength are improved when there are samples over several pings from the same fish (Ehrenberg and Torkelson, 1996; Foote *et al.*, 1984), and tracking can be used to obtain behavioral observations relevant to the target strength estimation (Chu *et al.*, 2003; McQuinn and Winger, 2003). Consequently, improving our ability to track single individuals may lead to better TS estimates, and if bias in intensity is a concern, the quality could be controlled by track quality parameters like the J_{merge}, cf. the following discussion of track quality. Another effect of the traditional approach is that weak and low-quality targets are undetected, which is a problem when addressing the interindividual behavior issues mentioned in Sec. I. Here it is crucial that low-quality tracks are detected, to avoid false nearest-neighbor pairing. This is also important when investigating the spatial distribution from single-target observations, as in, e.g., Pedersen (1996); Trenkel *et al.* (2004). Consequently, the method presented here improves the feasibility of experiments that rely on our ability to resolve single targets, including TS estimation.

Target tracking is a large field with an extensive literature, and several methods have been described, see, e.g., Blackman and Popoli (1999) as a general reference. Other data-association methods include multiple-hypothesis tracking. This approach delays the decision on data association for several pings, and keeps track of the most likely target associations. This results in several combinations (hypotheses) of the targets. This is the recommended data-association method according to Blackman and Popoli (1999, Chap. 6). However, keeping track of several track-combination hypotheses when working with echo samples, as opposed to single targets, would yield a vast number of combinations. It is possible that the method could be refined to fit this approach, but the complexity would increase. Other approaches includes particle filtering, e.g., the probability-hypothesis-density (PHD) method. The PHD filter has been implemented for forward-scan sonar images (Clark and Bell, 2005), and one advantage of this approach is its ability to filter signals in high clutter, reducing the number of spurious measurements. However, data association, the main consideration in this paper, is not presently addressed in the PHD method.

The novelty in the present work is the track-before-detect approach. This implies the use of angle samples in the detection, not only for rejection in the SED algorithms and in subsequent tracking. This is achieved by treating each sample above a threshold as a single target, and allowing for several associations of samples to each prediction (track). The approach is simple, but some further consideration of why it works may be appropriate. Humans have a remarkable capability to extract information from images, and that is one of the reasons that tracking targets in intensity echograms by eye often performs better than automatic tracking. However, when we include both anglegrams and existing track predictions in addition to the intensity echogram, our ability is less superior because we have to interpret the information in several images simultaneously. The computer has no problem in handling this multidimensionality.

A. Parameter sensitivity and track quality

The method is very flexible, and calls for caution when setting the parameters. In general, one should start with the most sensitive parameters and progress to the less sensitive parameters. The threshold should initially be set low to not miss any targets, and should subsequently be increased if necessary. The N_n parameter indicating the number of samples needed to initiate a track should be approximately the number of samples per ping from each target (5 in test data I). This is dependent on the sampling interval, the pulse length, and the target size range. The track-initiation gate range parameter, r_0, should be set slightly higher than the resolution in range (9.4 and 1.2 cm, for test data I and II, respectively). The track gate, G, depends on the fish behavior, the background reverberation, and the density. The track-termination and track-rejection parameters should initially be set high and then decreased, if necessary. After the initial settings are decided, a subsample of the data should be used for tuning the parameters. The parameters, G and G_0 should be tuned first. A larger initiation gate starts the tracks earlier, but potentially gives more false targets. If the track-initiation gate is narrowed too much, track-split errors in range may occur. If the track gate is increased, more rapid changes in behavior may be detected but several targets may be erroneously associated within one track, both in time and range. If the track gate is decreased, tracks may split and rapid changes in behavior will be undetected, but there will be less false associations. The track-termination and track-rejection parameters should be set to terminate and reject more tracks if the gate tuning does not improve the performance.

The performance of the tracker depends on the parameter values, and the above-outlined setting procedure involves subjectivity. An important aspect of the track-quality algorithm is to remove some of this subjectivity. As mentioned earlier, the definition of high or low quality may depend on the application, and these trade-offs can be achieved by different weights on the various quality measures. Further, a low-quality track may convert to a high-quality track by tuning the tracking parameters correctly, while the definition of track quality remains the same. Consequently, the track quality indicates the comparative success of the different parameter settings, but is also an absolute (as opposed to rela-

tive) measure of the track quality. This distinction is important because it gives us the possibility to assess whether tracking is feasible or not in a given situation, beyond the information on how well the parameters are set.

Although track quality measures have been established, the ultimate test is to visually compare the automatic classification into tracks with the appearance of the echogram and the anglegrams. The value of carefully inspecting these should not be underestimated, because humans are highly skilled at extracting information from images. Some researchers argue that manual tracking is better and more accurate than automatic tracking. Although this may be true in some cases, the manual approach is less consistent. Manual tracking may yield different results depending on who scrutinizes the data. Algorithms with given parameter settings do not have this problem.

B. Track estimation

An important part of any tracking system is the track-estimation process. Here, track estimation is defined as the information one can obtain from the samples comprising a single track, e.g., the estimated positions, the corresponding velocities, TS, etc. For example, if swimming velocities are required, simply dividing the distance between target fixes by the time difference is not good enough, because the observation errors are ignored, cf. Mulligan and Chen (2000) for a convincing illustration. Although this paper focuses on data association, a short discussion of different track estimation techniques is included.

The Kalman filter is a common method for estimating speed and positions in tracking applications. This is a powerful tool when real-time tracking is required, e.g., in the data association process when predictions are needed or when tracking airplanes or missiles. When estimating fish swimming trajectories, however, we can estimate the tracks after association. This enables us to use a whole suite of estimation techniques. Several methods have been tested on split-beam data in Handegard *et al.* (2005). Both smoothing splines and Kalman smoothing (Kalman smoothing traverse the Kalman filter estimates backwards to reduce dependence of the initial conditions) were found to work well for position estimates, but the Kalman smoother failed to estimate the velocities. In the test cases presented here, however, the Kalman smoother produced sensible results. If the process and measurement errors are well known, the Kalman smoother is an appropriate tool since it separates the process and observation errors, i.e., it reduces the number of *ad hoc* parameters. Another approach is to use smoothing splines where the smoothing is set by cross validation. For the test data in this paper, the cross-validation method detected periodicity in the position estimates. This has the potential to give grossly overestimated swimming-speed estimates if not corrected for. The importance of plotting the tracks to assess this effect should not be underestimated. However, the periodicity is believed to be caused by the tail-beat frequency of individual fish, and this could potentially be associated with the swimming speed (Bainbridge, 1960).

Another aspect, not addressed in this paper, is the quality of the angle measurements in each sample. This should be considered when estimating fish position and velocity. For example, low signal-to-noise ratio gives higher variability in the angles, but may also bias them toward the center of the beam (Kieser *et al.*, 2000). This is especially important when using sonars close to boundaries, as would apply in a riverine environment or with horizontal transmissions near the bottom or the water surface.

V. CONCLUSIONS

The main advantages of tracking samples directly without prior target detection are simplicity and efficiency. The process is simple, because no prior detection is necessary as the process of tracking and detection is done in one step. The efficiency is improved by the target angles being utilized along with the intensity and range data, as opposed to the conventional SED algorithm that works on intensity and range only. The benefit of this approach has been clearly demonstrated.

The combination of the improved data association and the quality control substantially improves our ability to investigate the behavior of closely spaced single targets, providing the means to learn more about the behavior of the individual animals within aquatic ecosystems.

ACKNOWLEDGMENTS

This work was carried out during a stay at the University of Washington and NOAA Alaska Fisheries Science Center, Seattle, funded by the Norwegian Research Counsel under the Leiv Erikson program. I would like to thank Egil Ona and Lucio Calise for the test data sets I and II, respectively, Karl Øystein Gjelland for processing the SONAR 5 data, and Vidar Hjellvik, Alex De Robertis, and Patrick H. Ressler for comments on the manuscript.

[1]I use the term "anglegram" to describe a ping-by-ping display of targets which are color-coded to indicate one of the bearing angles.
[2]Personal communication, based on camera observations of fish in a tank.

Aoki, I. (**1982**). "A simulation study on the schooling mechanism in fish," Bull. Japanese Soc. Sci. Fisheries **48**, 1081–1088.
Arrhenius, F., Benneheij, B. J., Rudstam, L. G., and Boisclair, D. (**2000**). "Can stationary bottom split-beam hydroacoustics be used to measure fish swimming speed in situ?," Fisheries Research **45**, 31–41.
Bainbridge, R. (**1960**). "Speed and stamina in three fish," J. Exp. Biol. **37**, 129–153.
Balk, H., and Lindem, T. (**2000**). "Improved fish detection in data from split-beam transducers," Aquatic Living Resources **13**, 297–303.
Blackman, S. S., and Popoli, R. (**1999**). *Design and Analysis of Modern Tracking Systems* (Artech House, Boston).
Brede, R., Kristensen, F. H., Solli, H., and Ona, E. (**1990**). "Target tracking with a split-beam echo sounder," Rapp. P.-v. Reun.-Cons. Int. Explor. Mer **189**, 254–263.
Breder, C. M. J. (**1954**). "Equations descriptive of fish schools and other animal aggregations," Ecology **35**, 361–370.
Cech, M., and Kubecka, J. (**2002**). "Sinusoidal cycling swimming pattern of reservoir fishes," J. Fish Biol. **61**, 456–471.
Chu, D., Jech, J. M., and Lavery, A. (**2003**). "Inference of geometrical and behavioural parameters of individual fish from echo-trace-analysis," Deep-Sea Res., Part I **50**, 515–527.
Clark, D., and Bell, J. (**2005**). "Bayesian multiple target tracking in forward scan sonar images using the phd filter," IEE Proc., Radar Sonar Navig. **152**, 327–334.

Craig, R. ed. (**1984**). ICES Symposium on Fisheries Acoustics, Bergen, Norway, 1982, Rapp. P.-v. Reun.-Cons. Int. Explor. Mer **184**.
Cronkite, G. M., Enzenhofer, H. J., and Gray, A. P. (**2004**). "Split-beam sonar observations of targets as an aid in the interpretation of anomalies encountered while monitoring migrating adult salmon in rivers," Aquatic Living Resources **17**, 1–12.
De Robertis, A., Schell, C., and Jaffe, J. (**2003**). "Acoustic observations of the swimming behaviour of the euphasiid *Euphasia pacifica* Hansen," ICES J. Mar. Sci. **60**, 885–898.
Ehrenberg, J. E., and Torkelson, T. C. (**1996**). "Application of dual-beam and split-beam target tracking in fisheries acoustics," ICES J. Mar. Sci. **53**, 329–334.
Enzenhofer, H. J., Olsen, N., and Mulligan, T. J. (**1998**). "Fixed-location riverine hydroacoustics as a method of enumerating migrating adult pacific salmon: Comparison of split-beam acoustics vs. visual counting," Aquatic Living Resources **11**, 61–74.
Foote, K. G. (**1996**). "Coincidence echo statistics," J. Acoust. Soc. Am. **99**, 266–271.
Foote, K. G., Aglen, A., and Nakken, O. (**1986**). "Measurement of fish target strength with a split-beam echo sounder," J. Acoust. Soc. Am. **80**, 612–621.
Foote, K. G., Kristensen, F. H., and Solli, H. (**1984**). "Trial of a new, split-beam echo sounder," Coun. Meet. Int. Coun. Explor. Sea B:21, Copenhagen, Denmark.
Genin, A., Jeffe, J. S., Reef, R., Richter, C., and Franks, P. J. S. (**2005**). "Swimming against the flow: A mechanism of zooplankton aggregation," Science **308**, 860–862.
Gjelland, K. Y., Bøhn, T., Knudsen, F. R., and Amundsen, P.-A. (**2004**). "Influence of light on the swimming speed og coregonids in subarctic lakes," Ann. Zool. Fennici **41**, 137–146.
Handegard, N. O., Michalsen, K., and Tjøstheim, D. (**2003**). "Avoidance behaviour in cod (*gadus morhua*) to a bottom-trawling vessel," Aquatic Living Resources **16**, 265–270.
Handegard, N. O., Patel, R., and Hjellvik, V. (**2005**). "Tracking individual fish from a moving platform using a split-beam transducer," J. Acoust. Soc. Am. **118**, 2210–2223.
Handegard, N. O., and Tjøstheim, D. (**2005**). "When fish meets a trawling vessel: Examining the behaviour of gadoids using a free floating buoy and acoustic split-beam tracking," Can. J. Fish. Aquat. Sci. **62**, 2409–2422.
Huse, I., and Ona, E. (**1996**). "Tilt angle distribution and swimming speed of overwintering norwegian spring spawning herring," ICES J. Mar. Sci. **53**, 863–873.
Huth, A., and Wissel, C. (**1992**). "The simulation of the movement of fish schools," J. Theor. Biol. **156**, 365–385.
Jaffe, J. S. (**1999**). "Target localization for a three-dimensional multibeam sonar imaging system," J. Acoust. Soc. Am. **105**, 3168–3175.
Jaffe, J. S., Ohman, M. D., and De Robertis, A. (**1999**). "Sonar estimates of daytime activity levels of *Euphausia pacifica* in Saanich Inlet," Can. J. Fish. Aquat. Sci. **56**, 2000–2010.
Jaffe, J. S., Reuss, E., McGehee, D., and Chandran, G. (**1995**). "FTV, a sonar for tracking macrozooplankton in 3-dimensions," Deep-Sea Res., Part I **42**, 1495–1512.
Karp, W., ed. (**1990**). ICES Symposium on Developments in Fisheries Acoustics, Seattle, WA, 1987, Rapp. P.-v. Reun. Cons. Int. Explor. Mer **189**.
Kieser, R., Mulligan, T., and Ehrenberg, J. (**2000**). "Observation and explanation of systematic split-beam angle measurement errors," Aquatic Living Resources **13**, 275–281.
Klevjer, T. A., and Kaartvedt, S. (**2003**). "Split-beam target tracking can be used to study the swimming behaviour of deep-living plankton in situ," Aquatic Living Resources **16**, 293–298.
MacLennan, D. N., Massé, J., and Gerlotto, F., eds. (**2003**). Sixth ICES Symposium on Acoustics in Fisheries and Aquatic ecology, Part 1, Montpellier, France, 2002, ICES J. Mar. Sci. **60**.
Margetts, A., ed. (**1977**). ICES Symposium on Hydro-Acoustics in Fisheries Research, Bergen, Norway, 1973, Rapp. P.-v. Reun. Cons. Int. Explor. Mer **170**.
Massé, J., Gerlotto, F., and MacLennan, D. N., eds. (**2003**). Sixth ICES Symposium on Acoustics in Fisheries and Aquatic ecology, Part 2, Montpellier, France, Aquatic Living Resources **16**.
McKinstry, C. A., Simmons, M. A., Simmons, C. S., and Johnson, R. L. (**2005**). "Statistical assessment of fish behavior from split-beam hydroacoustic sampling," Fisheries Research **72**, 29–44.
McQuinn, I., and Winger, P. (**2003**). "Tilt angle and target strength: Target tracking of atlantic cod (gadus morhua) during trawling," ICES J. Mar. Sci. **60**, 575–583.
Mulligan, T., and Chen, D. (**2000**). "Comment on 'can stationary bottom split-beam hydroacoustics be used to measure fish swimming speed in situ?' by Arrhenius *et al.*," Fisheries Research **49**, 93–96.
Mulligan, T. J., and Chen, D. G. (**1998**). "A split-beam echo counting model: Development of statistical procedures," ICES J. Mar. Sci. **55**, 905–917.
Mulligan, T. J., and Kieser, R. (**1996**). "A split-beam echo-counting model for riverine use," ICES J. Mar. Sci. **53**, 403–406.
Ona, E. (**1994**). "Recent developments of acoustic instrumentation in connection with fish capture and abundance estimation," in *Marine Fish Behaviour in Capture and Abundance Estimation*, edited by A. Fernö and S. Olsen (Fishing News Books, Oxford, UK), pp. 200–214.
Ona, E., ed. (**1999**). "Methodology for Target Strength Measurements," ICES Cooperative Research Report (International Council for the Exploration of the Sea), Vol. **235**.
Parr, A. E. (**1927**). "A contribution to the theoretical analysis of the schooling behaviour of fishes," Occasional Papers of the Bingham Oceanographic Collection **1**, 1–32.
Pedersen, J. (**1996**). "Discrimination of fish layers using the three-dimensional information obtained by a split-beam echo-sounder," ICES J. Mar. Sci. **53**, 371–376.
Reynolds, C. W. (**1987**). "Flocks, herds, and schools: A distributed behavioural model," Comput. Graphics **21**, 25-34.
Sakai, S. (**1973**). "A model for group structure and its behaviour," Biophysics (Engl. Transl.) **13**, 82–90.
Schell, C., and Jaffe, J. S. (**2004**). "Experimental verification of an interpolation algorithm for improved estimates of animal position," J. Acoust. Soc. Am. **116**, 254–261.
Simmonds, E. J., ed. (**1996**). ICES Symposium on Fisheries and Plankton Acoustics, Aberdeen, Scotland, 1995, ICES J. Mar. Sci. **53**.
Soule, M., Hampton, I., and Barange, M. (**1996**). "Potential improvements to current methods of recognizing single targets with a split-beam echo-sounder," ICES J. Mar. Sci. **53**, 237–243.
Torgersen, T., and Kaartvedt, S. (**2001**). "In situ swimming behaviour of individual mesopelagic fish studied by split-beam echo target tracking," ICES J. Mar. Sci. **58**, 346–354.
Trenkel, V. M., Godø, O. R., Handegard, N. O., and Patel, R. (**2004**). "Studying the relationship between spatial fish distributions and trawl catches," Coun. Meet. Int. Coun. Explor. Sea R:26, Copenhagen, Denmark.
Xie, Y. (**2000**). "A range-dependent echo-association algorithm and its application in split-beam sonar tracking of migratory salmon in the fraser river watershed," IEEE J. Ocean. Eng. **25**, 387–398.

ICES Journal of Marine Science, 60: 524–531. 2003
doi:10.1016/S1054–3139(03)00032-8

Inferring fish orientation from broadband-acoustic echoes

Timothy K. Stanton, D. Benjamin Reeder, and J. Michael Jech

Stanton, T. K., Reeder, D. B., and Jech, J. M. 2003. Inferring fish orientation from broadband-acoustic echoes. – ICES Journal of Marine Science, 60: 524–531.

A new method has been developed for inferring the orientation of fish through the use of broadband-acoustic signals. The method takes advantage of the high range resolution of these signals, once temporally compressed through cross-correlation. The temporal resolution of these compressed signals is inversely proportional to the bandwidth, thus the greater the bandwidth the higher the resolution. This process has been applied to broadband-chirp signals spanning the frequency range 40–95 kHz to obtain a range resolution of approximately 2 cm from the original, unprocessed resolution of about 50 cm. With such high resolution, individual scattering features along the fish have been resolved, especially for angles well off normal incidence. The overall duration of the compressed echo from live, individual alewife, as measured in a laboratory tank, is shown to increase monotonically with orientation angle relative to normal incidence. The increase is due to the greater range separation relative to the transducer between the echoes from the head and tail of the fish. The results of this study show that with *a priori* knowledge of the length of the fish, the orientation could be estimated from the duration of a single, compressed broadband echo. This method applies to individual, acoustically resolved fish. It has advantages over previous approaches because it derives the orientation from a single ping and it does not use a formal, mathematical scattering model. Design parameters for applications in the ocean are given for a range of conditions and fish size.

Keywords: acoustic scattering, broadband acoustics, fish.

T. K. Stanton, and D. B. Reeder: Department of Applied Ocean Physics and Engineering; Woods Hole Oceanographic Institution, 98 Water Street, MS #11; Woods Hole, MA 02543, USA. J. M. Jech: Northeast Fisheries Science Center; 166 Water Street; Woods Hole, MA 02543, USA; tel: +1 508 495 2353; fax: +1 508 495 2258; e-mail: michael.jech@noaa.gov. Correspondence to T. K. Stanton; tel: +1 508 289 2757; fax: +1 508 457 2194; e-mail: tstanton@whoi.edu.

Introduction

It is important to know the distribution of the orientations of free-swimming fish for two reasons. First, the orientation distribution of fish correlates with the type of behavior the animal is exhibiting, such as feeding or migrating. Knowledge of the orientation distribution under a variety of conditions will therefore contribute to the fundamental understanding of animal behavior. Second, acoustics is commonly used as a means to survey fish rapidly and synoptically. Since acoustic scattering depends strongly upon the orientation of the fish, knowledge of its distribution will help to quantify interpretation of the acoustic-survey data.

Measurement of the orientation of fish is a challenge. The most direct method involves use of cameras (Huse and Ona, 1996). However, this is logistically difficult, involves a small sampling volume, and can induce avoidance reactions that would contaminate the data. Acoustic-scattering techniques are less invasive and involve a much larger sampling volume. One acoustical method has involved tracking individual fish over multiple pings, either directly or through echo-trace analysis, and equating orientation angle to swim angle (Furusawa and Miyanohana, 1990; Ona, 2001). Another method has involved inferring the orientation, or its distribution, from the scattering data using an assumed scattering model (Foote and Traynor, 1988; Chu *et al.*, 1993; Martin Traykovski *et al.*, 1998).

Clearly, it is most desirable, if possible, to use a synoptic, non-invasive method to measure orientation with the fewest assumptions and least data. Broadband-acoustic signals offer advantages for the inference of orientation. A genuinely broadband signal, i.e. one with a bandwidth of approximately one octave or greater, is rich with information as it spans continuously a broad range of frequencies. Because of this inherent property, there is potential for reducing the number of ambiguities in the interpretation of the data. The challenge is in the selection of the optimal approach.

1054–3139/03/000524+08 $30.00

In this paper, we propose a new method that uses broadband-acoustic signals to infer remotely the orientation of individual fish. We take advantage of a pulse-compression technique in which the duration of the received echo is reduced significantly so that individual features of the fish can be resolved in the time domain (Chu and Stanton, 1998; Stanton *et al.*, 1998). The orientation of the fish can be estimated through simple, geometric arguments and *a priori* knowledge of the length of the fish. The information on the (resolved) fish can be extracted from a single ping. Although a formal, mathematical-scattering model is not required in the analysis, it is assumed that there are scattering features distributed along the entire length of the fish and centered about the lengthwise axis of the fish. These features need to produce echoes of sufficient strength for detection. We present broadband (40–95 kHz), acoustic-backscattering data collected in the laboratory, where the scattering was measured as a function of the angle of orientation for a number of individual fish. The duration of the series of detectable, compressed echoes for each ping is shown to increase monotonically with the angle of orientation over a wide range of angles. Furthermore, the echoes are linked directly to scattering features along the length of the fish. A simple, geometry-based equation is used to describe this relationship and is used to predict sonar performance for a range of system parameters for use in the ocean.

Pulse-compression processing of broadband signals

Basic properties

The pulse-compression processing used here has been applied to acoustic-backscattering data involving fish by Ehrenberg and Torkelson (2000) and Reeder *et al.* (accepted for publication), and to zooplankton backscattering data by Stanton *et al.* (1998) and Chu and Stanton (1998). The processing is based on, and is quite similar to, the commonly used, matched-filter processing. Matched-filter processing was developed to optimize the detection of a known signal in the presence of random noise (Turin, 1960). It has since been used in a variety of applications, including acoustic propagation and scattering in the ocean (Medwin and Clay, 1998). In the matched-filter approach, the noisy signal is cross-correlated with the known or noiseless signal. Given sufficient bandwidth and a known signal of sufficient duration such as a chirp, matched-filter processing results in a signal with much higher amplitude and shorter duration than the original signal (Figure 1). The shape of the processed signal is characterized by a single, high-amplitude main lobe with smaller side lobes corresponding to artifacts of the processing. Since this process increases the amplitude of the signal but not the (non-reverberative) noise, the result of applying the matched filter to a noisy signal significantly increases the signal-to-noise ratio (SNR). Also, the width of the main lobe is inversely proportional to the bandwidth of the original signal, greatly increasing the possible temporal resolution. For example, the width of a processed 600-μs-long chirp signal spanning the frequency range 40–95 kHz is about 20 μs. For underwater-acoustic signals, this corresponds to an improvement in range resolution from about 50 cm to about 2 cm.

Application to acoustic scattering by marine life

There are significant advantages associated with processing broadband echoes in a manner similar to that of matched-filter processing. One, as discussed above, is that the SNR is improved, which allows detection of targets at greater ranges. Furthermore, the range resolution is improved, which allows targets at greater numerical densities to be resolved. The challenge lies in both the implementation of the algorithm and the interpretation of the processed signal. Since the target affects the properties of the incident acoustic wave because of its inherent scattering properties, the ideal, noiseless signal with which the received echo should be cross-correlated is not known. This problem has been addressed by simply using the transmission or calibration signal as the so-called "replicate" signal. The resulting "compressed pulse", although different from what a true matched-filter would produce, has the same advantages of increased SNR and decreased duration, although to a lesser degree. The increase in SNR, using pulse-compression processing has been demonstrated both for fish (Ehrenberg and Torkelson, 2000; Reeder *et al.*, accepted for publication) and zooplankton (Chu and Stanton, 1998; Stanton *et al.*, 1998).

A useful consequence of the fact that the cross-correlated, scattered signal deviates from a matched filter is the information contained in that deviation. The resulting signal from a matched filter is a single, short spike with small side lobes (Figure 1, lower-right panel). The shape of this signal is what one would expect when the signal had been scattered by a target that is smaller than the compressed range resolution and possesses a uniform-frequency response. However, for an extended biological target, the cross-correlated, scattered signal will, in general, comprise a series of spikes corresponding to the various scattering features of the scattering object (Chu and Stanton, 1998; Stanton *et al.*, 1998; Barr, 2001; Reeder *et al.*, accepted for publication). These scattering features are resolved through the inherent increase in resolution of the cross-correlated signal and through an appropriate combination of bandwidth and animal size. Animals such as fish contain anatomical variations throughout the length of the body. These variations cause acoustic scattering and, for long pings, there are generally contributions from structure within the entire body to the total received (unprocessed) echo. Once the echo is compressed, echoes due to various features will be separated in time, especially for oblique

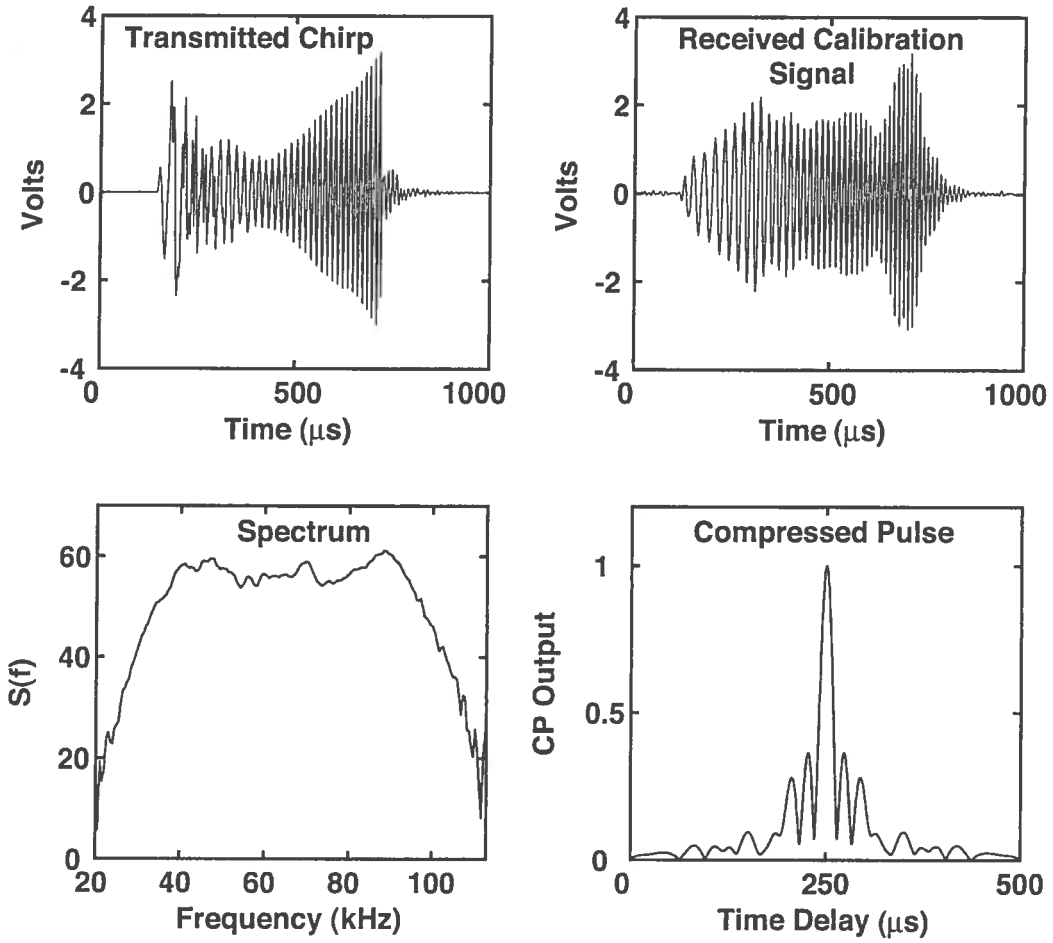

Figure 1. Broadband-acoustic signals. (Upper-left panel) Shaped, chirp signal as applied to the transmitting transducer. This signal was used in both the scattering and the calibration measurements. (Upper-right panel) Signal at output of the receiving transducer in the calibration setup with the transmitting transducer using the same signal as illustrated in the upper left panel and aimed at the receiving transducer. (Lower-left panel) Frequency spectrum of signal (in dB) at output of the receiver transducer in the calibration setup. (Lower-right panel) Envelope of the autocorrelation function, corresponding to matched-filter output, of the received signal from the upper-right panel. The great reduction in pulse duration of the compressed pulse relative to the applied chirp in the upper-left panel is illustrated. The amplitude is normalized to unity.

angles (Figure 2). For angles near normal incidence, the echoes from the various features will tend to arrive at approximately the same time. However, as the angle departs significantly from normal incidence, the times of arrivals will deviate according to the orientation of the fish relative to the direction of the incident wave.

For a sufficiently short, compressed pulse, an orientation angle well away from normal incidence, and given a long enough fish, the arrivals can be resolved. The separation in time, $\Delta\tau$, between the first and last arrival can be determined approximately through simple geometry:

$$\Delta\tau = (2L_{eff}/c)\,|\cos\theta| \qquad (1)$$

where c is the speed of sound in water, L_{eff} is the effective acoustic length of the fish, and θ is the angle between the direction of propagation of the incident acoustic signal and the lengthwise axis of the fish (e.g. for tail-on incidence, $\theta = 0°$; normal incidence, $\theta = 90°$; head-on incidence, $\theta = 180°$). This coordinate system is convenient for analyzing data over the full range of angles of incidence in a given plane of rotation (0–360°). For the coordinate system involving the commonly used "tilt angle", which is the angle of the fish axis relative to the horizontal plane, that angle is equal to θ–90° for the case of a downwards-looking echosounder. In the above equation, $\cos\theta$ would be replaced by sin (tilt angle). Also, as discussed above, ideally there would be significant sources of scattering along the entire length of the fish. Since, generally, there are no significant anatomical variations at the tail of the fish, the effective length L_{eff} is used to describe the length of the line of scattering features. As described below, for the alewife used in this study, L_{eff} is about 90–95% of the actual length of the fish.

The above equation relates the orientation of the fish to the temporal extent of the processed acoustic echo. It is

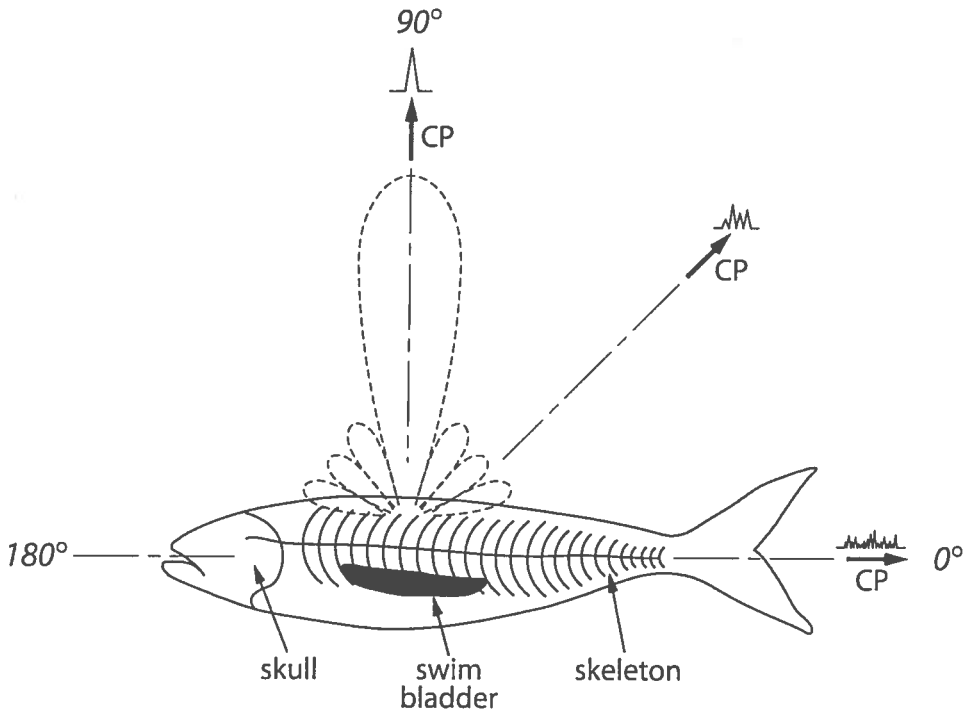

Figure 2. A schematic illustration of a compressed echo or pulse (CP) as a function of backscatter direction. The duration of the pulse is short for near-normal incidence and longer for oblique angles. The characteristics of the compressed pulse are illustrated for three values of θ (0, 45, and 90°).

very simple and relies principally on knowledge of the length of the fish and the duration, i.e. the time between first and last arrival of the processed echo. This relationship will be explored through the analysis of laboratory data in the next section. Specifically, the relationship will be examined in terms of the inherent limitations of a finite-bandwidth, acoustic system as well as deviations of the fish from an idealized line scatterer. These deviations include the facts that the organs or scattering features that give rise to significant echoes do not necessarily extend along the full length of the fish, are finite in size, and are not necessarily co-linear.

Experiments

A series of measurements of broadband-acoustic backscattering by live, individual fish has recently been completed (Reeder *et al.*, accepted for publication). The laboratory measurements were conducted in a $6 \times 6 \times 6\ m^3$ tank filled with fresh water, using alewife (*Alosa pseudoharengus*), a swimbladder-bearing fish similar to Atlantic herring (*Clupea harengus*). The 17 fish, all ensonified separately, were similar in length with an average caudal length (i.e. the length measured between the nose and the end of the flesh near the tail) of approximately 22 cm. All measurements involved the use of a pair of closely spaced, broadband transducers, one used as a transmitter and the other a receiver. A shaped, linearly-swept, frequency-modulated signal (chirp) spanning the frequency range 40–95 kHz was used. The scattering was measured over all angles of orientation (1° increments) in two planes of rotation as the tethered fish were rotated within the acoustic beam. The anatomy and morphology of the fish were characterized through a combination of physical measurement, dissection, traditional X-rays, computerized-tomography (CT) scans, and phase-contrast X-rays. Details of the experiments and results are presented in Reeder *et al.* (accepted for publication) and a preliminary report of their pulse-compression results is given in Stanton *et al.* (2001).

A particularly noteworthy result of the experiment was the ability of the system to resolve individual scattering features along the length of the body of the fish (Figures 3 and 4). As reported earlier in the article, the range resolution of the unprocessed 600-μs ping for this laboratory system was approximately 50 cm and after pulse compression it was about 2 cm. For the 22-cm long fish with major features, such as the skull and swimbladder separated by more than 2 cm, several features were acoustically resolved in the compressed pulse, especially at angles well away from normal incidence. The general characteristics of all data were broadly similar: the compressed pulse was a short, single spike near normal incidence (dorsal/ventral plane or lateral plane), but once the orientation was well

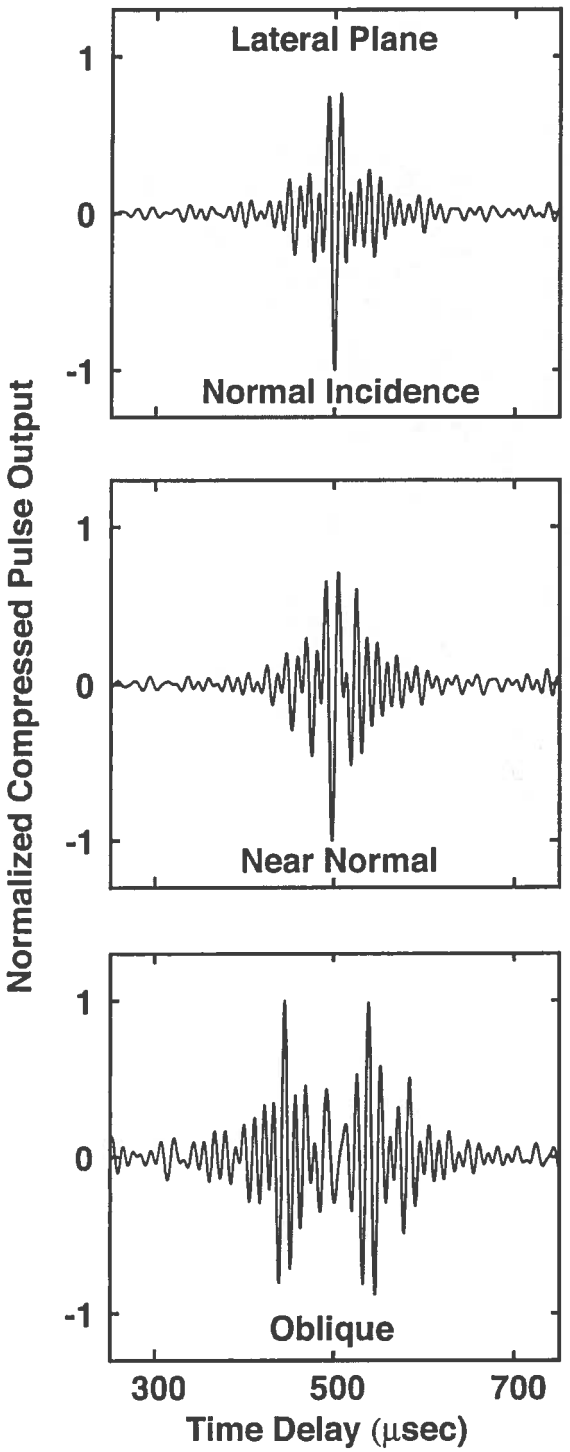

Figure 3. Compressed pulses from the echoes measured from an alewife at three orientation angles in the lateral plane. "Near normal" and "oblique" incidence correspond to angles that were 5 and 60° off-normal incidence, respectively. At the oblique angle, the echo comprises two major resolved peaks. Time delays (horizontal-axis) are relative to 5 ms, thus a time delay of 300 μs corresponds to 5.3 ms after the initial transmission.

away from normal, the single spike separated into a series of peaks. These observations are consistent with the fact that echoes from scattering features along the body will arrive at approximately the same time at angles near normal incidence. Once the orientation is well away from normal incidence, anatomical features closer to the transducers will produce echoes that arrive sooner than the features at the far end of the body.

All the data showed the trend of monotonic increase in separation between the first and last arrival ($\Delta\tau$) relative to orientation angle for angles out to 40–50° from normal incidence (Figure 4). Although Equation (1) generally accounts for this trend over that range, the scatter of points increases with increasing angle toward end-on incidence (Figures 5 and 6). At angles near end-on (tail-on or head-on), the relationship between orientation angle and peak separation is more complicated and Equation (1) does not describe the separation adequately. The increasing deviation between the data and model is due to the fact that with near end-on incidence, the echoes from the scattering features at the far side of the body are shadowed and therefore possibly not detected. However, since there is no or little shadowing for angles closer to normal incidence, and given the consistency of the data in that region, there is potential for extracting orientation information from the time signature of the compressed-pulse output.

Recommendations for field applications

These data show a trend of monotonic increase in the time separation between the first and last arrivals of the compressed-pulse output as the orientation angle near normal incidence deviates away from normal incidence (Figures 5 and 6). Given this consistency, there is potential for extracting orientation information from a processed broadband echo. A few questions remain regarding the accuracy and precision of the results and the optimal design of an acoustic system to take advantage of such a method. The answers involve the bandwidth of the system, the distribution of the scattering features with respect to position (length- and depth-wise) within the fish, and artifacts in the echo due to scattering-related interference phenomena.

Although there is a general trend of monotonic increase in the time separation between the first and last echoes with angle of orientation near normal incidence, there is variability about that trend. There are several possible causes of that spread, one being related to the experimental approach. This experiment involved live fish constrained in an acoustically-transparent harness. The harness was made tight enough to constrain the fish within the acoustic beam but loose enough so as not to cause too much stress on the fish during the measurements. Movement of the fish was apparent in some of the data (not shown). It is reasonable to believe that, although the harness was rotated in 1° increments, the fish may have moved at least that much

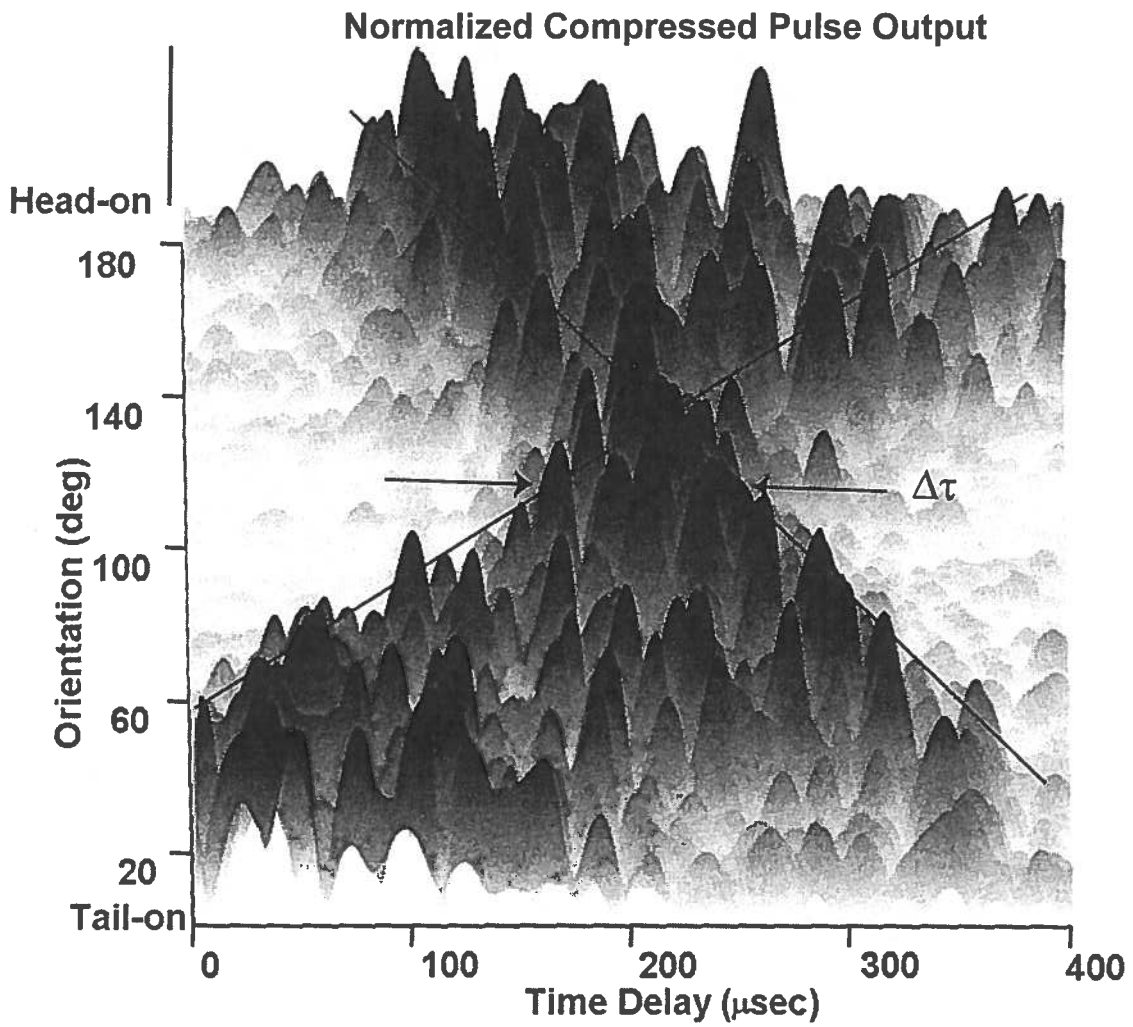

Figure 4. Envelopes of compressed echoes for a range of orientation angles (θ) from an alewife that was rotated in the dorsal/ventral plane. The straight lines are drawn to illustrate the trends of the locations of the leading and trailing edges of the first and last arrivals, respectively. The minimum value of $\Delta\tau$ occurs near 90° (normal incidence), although it has the appearance of occurring at a larger angle due to the perspective of this three-dimensional plot. Time delays (horizontal-axis) are relative to 5 ms, thus a time delay of 0 μs corresponds to 5 ms after the initial transmission.

in the course of the measurement and thus cause error in the reported value of orientation.

Other sources of variability involve the location of the scattering features and interference between them. This is not a laboratory artifact and will occur in the natural ocean environment. Our model assumes that the scattering features in the fish are all located along its lengthwise axis and that there are scattering centers at both ends of the fish. Thus at normal incidence, the associated echoes would all arrive at precisely the same time. However, anatomical features are distributed throughout the depth of the body of the fish and these scattering features vary in thickness. The composite effect of these two facts results in echoes that arrive at *approximately*, but not exactly, the same time when the fish is at normal incidence. This variation is bounded by the thickness of the fish and will certainly be associated with a small fraction of the thickness. Furthermore, because of interference between the arrivals, there will be some variation in the leading or trailing edge of the first and last arrivals, respectively, of the compressed pulse, causing further distortion of the results. The error associated with this interference will be bounded by the temporal resolution of the compressed pulse. Finally, significant scattering may not necessarily arise from parts of the fish near the tail, resulting in an effective acoustic length for use in Equation (1) that is shorter than the true length. If not taken into account, the error in the inferred angle of orientation would be approximately 5–10% for the fish and the acoustic parameters used in our study.

One important limiting factor in this approach involves the bandwidth, since this dictates the temporal resolution of the process. As mentioned above, the resolution is inversely

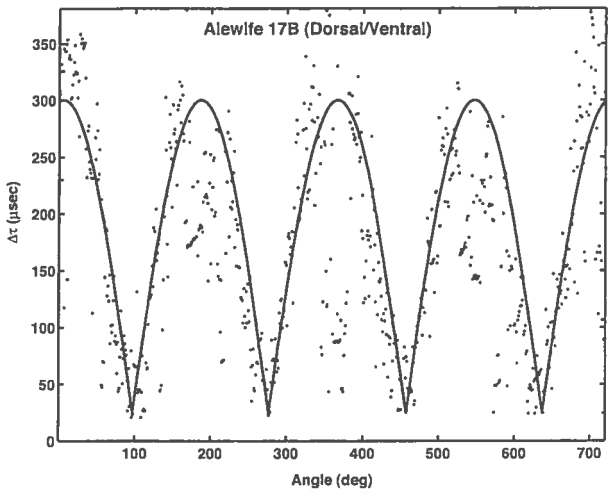

Figure 5. The time difference between the beginning of the first arrival of the compressed-pulse echo and the end of the last arrival for a superset of the orientation angles (θ) shown in Figure 4. The alewife was rotated through 720°. Detection criteria for these outer tails of the time-series involved starting or stopping the count when the time-series reached 40% of the maximum level for a given orientation angle. This detection threshold was chosen to be just above the processing side lobes of the autocorrelation function of the calibration signal as shown in Figure 1 in order to ensure that each compressed pulse represents an actual echo and is not a processing artifact. Equation (1) is superimposed for comparison (with offsets), using an effective acoustic length of 90% of the measured caudal length. The horizontal offset is incorporated to account for deviations of the fish from an ideal line scatterer—which could cause additional time shifts—as well as the possible misalignment of the fish in the measurement. The vertical offset accounts for the bandwidth and hence finite temporal resolution of the acoustic system.

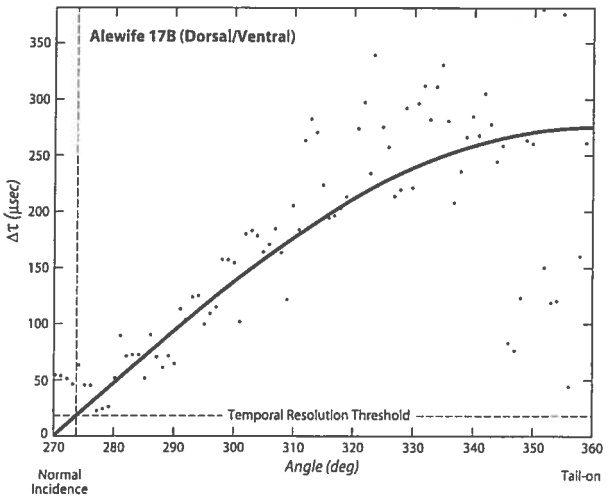

Figure 6. An expanded plot of one angular section of Figure 5. The minimum angle of inference relative to normal incidence (vertical dashed line) corresponds to the inverse bandwidth or minimum compressed-pulse width of the signal (horizontal dashed line). The effective acoustic length used in Equation (1) is 95% of the measured caudal length. The small difference in the effective acoustic length between this plot and that in Figure 5 is attributed to the fact that different sections of data were used and there are random differences between the two sections, as well as the fact that no vertical offset was used for Equation (1).

proportional to bandwidth of the signal. It is therefore important to use a system with a high bandwidth. The 2-cm range resolution of the processed echo in the system described in this article resulted in a detection threshold of about 4° relative to normal incidence for the 22-cm-long fish (e.g. the 274° point in Figure 6). Increasing the bandwidth of the system would decrease the threshold to the point where other limitations involving the non-co-linear nature of scattering features become important.

The choice of bandwidth of the system should therefore be based on the expected size of fish and corresponding deviations of scattering features from a straight line, and the desired threshold of detection of orientation angle relative to normal incidence (Table 1). It is important to stress that the criteria involving bandwidth are independent of the particular frequencies involved (e.g. a 100 kHz bandwidth could be derived from a 50–150 kHz system or a 150–250 kHz system). Since it is easier to fabricate efficient high-bandwidth systems at higher frequencies because the corresponding *fractional* bandwidth is smaller, then the trade-off between higher frequencies and shorter ranges of detection must be considered: signals at higher frequencies travel shorter distances.

Finally, for a practical field system, the effects of the beam pattern must somehow be accounted for, since beam widths are a strong function of frequency. This can, in principal, be accomplished by several methods. One, using conventional technology, could involve the simultaneous use of a narrow-band, split-beam echosounder co-located with a broadband, single-beam system. The split-beam system could be used to locate the position of the fish in the single beam and the effects of the beam pattern of the single beam could be removed. More advanced approaches could involve the development of a broadband, split-beam system or a system with a frequency-independent beam width.

Table 1. The bandwidth required for a range of minimum, inferred orientation angles relative to normal incidence and two lengths for an ideal line scatterer. The bandwidth was calculated using the approximate relationship, bandwidth $\simeq (\Delta\tau)^{-1}$ and Equation (1). The minimum angles for a fish will be larger because of effects such as the non-co-linearity of scattering features.

Minimum angle (deg)	Length (cm)	Bandwidth (kHz)
3	20 (40)	72 (36)
5	20 (40)	43 (21.5)
10	20 (40)	22 (11)
20	20 (40)	11 (5.5)

Summary and conclusion

We have conducted laboratory measurements of broadband scattering by swimbladder-bearing fish as a function of the angle of orientation. The temporally-compressed echoes had a 2-cm range resolution and were able to resolve individual scattering features within the fish. We observed that the time separation between the first and last returns of the compressed echoes was strongly correlated with the angle of orientation for a wide range of angles (normal incidence ±40°). Using this information, we conclude that the orientation of individual (resolved) fish can be inferred from the processed broadband echo from a single ping. Although some of the error in the inference is associated with artifacts of the laboratory measurement, e.g. movement of the fish within the harness and its imperfect alignment, there is also error associated with the non-co-linear nature of the scattering features along the length of the fish as well as interference between unresolved features. We recommend that the bandwidth be chosen to be as large as possible until the range resolution of the processed signal is comparable to the error associated with the non-co-linearity. Certainly, further assessment of the errors should involve free-swimming fish of various species with careful measurement of orientation.

In conclusion, broadband-acoustic signals are rich with information. As demonstrated in this article, one important quantity that can be inferred from a single ping is the orientation of resolved fish. Advantages of this approach over others are that only one ping is required and a formal mathematical-scattering model is not required. The design criteria of such an acoustic system involve the trade-off of bandwidth and the desired threshold of orientation relative to normal incidence as well as the desired range of detection. The design must also take account of the non-co-linearity of features along the fish that are species-dependent.

Acknowledgements

This research was supported by the U.S. Navy, the U.S. Office of Naval Research (grant nos. N00014-98-1-0879 and N00014-00-F-0148), NOAA (cooperative agreement NA87RJ0445), and the Massachusetts Institute of Technology/Woods Hole Oceanographic Institution Joint Graduate Education program. We are grateful to Robert Kieser of the Pacific Biological Station, Nanaimo, BC for his helpful suggestions. This is Woods Hole Oceanographic Institution contribution number 10788.

References

Barr, R. 2001. A design study of an acoustic system suitable for differentiating between orange roughy and other New Zealand deep-water species. Journal of the Acoustical Society of America, 109: 164–178.

Chu, D., and Stanton, T. K. 1998. Application of pulse compression techniques to broadband acoustic scattering by live individual zooplankton. Journal of the Acoustical Society of America, 104: 39–55.

Chu, D., Foote, K. G., and Stanton, T. K. 1993. Further analysis of target strength measurements of Antarctic krill at 38 kHz and 120 kHz: comparison with deformed cylinder model and inference of orientation distribution. Journal of the Acoustical Society of America, 93: 2985–2988.

Ehrenberg, J. E., and Torkelson, T. C. 2000. FM slide (chirp) signals: a technique of significantly improving the signal-to-noise in hydroacoustic assessment systems. Fisheries Research, 47: 193–199.

Foote, K. G., and Traynor, J. J. 1988. Comparison of walleye pollock target strength estimates determined from *in situ* measurements and calculations based on swimbladder form. Journal of the Acoustical Society of America, 83: 9–17.

Furusawa, M., and Miyanohana, Y. 1990. Behaviour and target-strength observation through echo traces of individual fish. Rapports et Procès-Verbaux des Réunions du Conseil International pour l'Exploration de la Mer, 189: 283–294.

Huse, I., and Ona, E. 1996. Tilt angle distribution and swimming speed of overwintering Norwegian spring spawning herring. ICES Journal of Marine Science, 53: 863–873.

Martin Traykovski, L. V., O'Driscoll, R. L., and McGehee, D. E. 1998. Effect of orientation on broadband acoustic scattering of Antarctic krill *Euphasia superba*: implications for inverting zooplankton spectral acoustic signatures for angle of orientation. Journal of the Acoustical Society of America, 104: 2121–2135.

Medwin, H., and Clay, C. S. 1998. Fundamentals of Acoustical Oceanography. Academic Press, Boston, 712 pp.

Ona, E. 2001. Herring tilt angles, measured through target tracking. *In* Herring: Expectations for a New Millennium, pp. 509–519. Ed. by F. Funk, J. Blackburn, D. Hay, A. J. Paul, R. Stephenson, R. Torenson, and D. Witherell. University of Alaska, Fairbanks, University of Alaska Sea Grant, AK-SG-01-04. Fairbanks.

Reeder, D. B., Jech, J. M., and Stanton, T. K. Broadband acoustic backscatter and high-resolution morphology of fish: measurement and modeling. Journal of the Acoustical Society of America (accepted for publication).

Stanton, T. K., Chu, D., and Wiebe, P. H. 1998. Sound scattering by several zooplankton groups. I. Experimental determination of dominant scattering mechanisms. Journal of the Acoustical Society of America, 103: 225–253.

Stanton, T. K., Chu, D., Martin Traykovski, L. V., Reeder, D. B., Warren, J. D., and Wiebe, P. H. 2001. Broadband acoustic classification of individual zooplankton and fish: a review of recent work. pp. 181–188 in Proceedings of the Institute of Acoustics Conference on Acoustical Oceanography, April 2001.

Turin, G. L. 1960. An introduction to matched filters. Institute of Radio Engineers Transactions on Information Theory, IT-6: 311–329.